Journal of Geotechnical and Geoenvironmental Engineering

Impact of suction and swell-induced softening on pile behavior in an unsaturated expansive clay

--Manuscript Draft--

Manuscript Number:	GTENG-13906R2
Full Title:	Impact of suction and swell-induced softening on pile behavior in an unsaturated expansive clay
Manuscript Region of Origin:	INDIA
Article Type:	Technical Paper
Manuscript Classifications:	Foundations; Geotechnical monitoring; Geotechnical structures
Funding Information:	Engineering and Physical Sciences Research Council (EP/P029434/1) — Ashraf S. Osman Commonwealth Scholarship Commission (INCN-2023-196) — Sonu Kumar
Abstract:	The study examines the response of a single pile embedded in an unsaturated expansive clay. This was achieved by performing three-dimensional finite element analyses, employing the Barcelona Basic Model. The study aimed to quantify the contribution of suction and swell-induced softening in dictating the mobilization of shaft resistance. Centrifuge testing was used as a benchmarking study to simulate the free swell and pile pull-out response. The resulting coupled hydro-mechanical flow deformation analyses effectively captured swell evolution, changes in lateral swell pressure and swell-induced softening, all of which significantly influenced load mobilization along the pile length. The results obtained identified zones of both positive and negative shaft resistance along the pile, previously overlooked by studies focusing solely on the development of positive resistance within the active zone. The development of tensile load in the pile was closely correlated with the reduction in suction and resulting swell upon wetting. During initial wetting, reduction of suction to the air occlusion value (where only 18% of total swell had been achieved) produced the maximum tensile load, after which reductions were observed. Furthermore, in comparison to rainfall infiltration, a rise in the water table was found to be a more critical hydraulic condition, generating maximum axial load and pile uplift. The study also highlighted conservatism in calculating pile capacity based on saturated soil mechanics, with the capacity found to be around five times lower than under unsaturated conditions. These findings enhance the understanding of pile foundation design in unsaturated expansive clays.
Corresponding Author:	Ashutosh Kumar, Ph.D. IIT Mandi: Indian Institute of Technology Mandi MANDI, Himachal Pradesh INDIA
Corresponding Author E-Mail:	ashutosh@iitmandi.ac.in;ashutoshkiit90@gmail.com
Order of Authors:	Sonu Kumar, M.Tech. Ashutosh Kumar, Ph.D. Tiago A.V. Gaspar, PhD Ashraf S. Osman, PhD
Additional Information:	
Question	**Response**
The journal requires that all submissions fall within its aims and scope, explained here. Please explain how your submission fits the journal's aims and scope.	The work presented within this manuscript highlights the importance of swell induced softening in dictating the response of single pile foundation embedded in unsaturated expansive clay. This was achieved by performing centrifuge testing, element testing and the numerical modelling. This study is related to foundation geomechanics and therefore it is within the scope of JGGE.

Powered by Editorial Manager® and ProduXion Manager® from Aries Systems Corporation

Papers published in ASCE Journals must make a contribution to the core body of knowledge and to the advancement of the field. Authors must consider how their new knowledge and/or innovations add value to the state of the art and/or state of the practice. Please outline the specific contributions of this research in the comments box.	The work presented within this manuscript examines the response of a single pile embedded in unsaturated expansive clay using centrifuge testing and numerical modelling. The numerical model employed Barcelona Basic Model (BBM) to model the clay with parameters calibrated through element-scale laboratory testing. The obtained results identified zones of both positive and negative shaft resistance along the pile length, previously overlooked by studies focusing solely on positive resistance development within the active zone that is the zone of water content fluctuation. The study also highlights that rise in the water table is more critical hydraulic condition, generating maximum axial load and pile uplift compared to rainfall infiltration condition. As per authors knowledge, this is the first time such detailed analysis are conducted on pile embedded in unsaturated expansive clay and therefore, the findings of this study will help in better understanding the behavior of pile foundation in such soil.
Authors are required to attain permission to re-use content, figures, tables, charts, maps, and photographs for which the authors do not hold copyright. Figures created by the authors but previously published under copyright elsewhere may require permission. For more information see ASCE Publication Policies. All permissions must be uploaded as a permission file in PDF format. Are there any required permissions that have not yet been secured? If yes, please explain in the comment box.	No
ASCE does not review manuscripts that are simultaneously under submission elsewhere. Is the article or parts of it being consideredfor any other publication? If your answer is yes, please explain in the comments box below.	No
Each submission to ASCE must stand on its own and represent significant new information, which may include disproving the work of others. While it is acceptable to build upon one's own work or replicate other's work, it is not appropriate to fragment the research to maximize the number of manuscripts or to submit papers that represent very small incremental changes. ASCE may use tools such as CrossCheck, Duplicate Submission Checks, and Google Scholar to verify that submissions are novel. Does the manuscript constitute incremental work (i.e. restating raw data, models, or conclusions from a previously published study)?	No
Authors are expected to present their papers within the page limitations	No

Powered by Editorial Manager® and ProduXion Manager® from Aries Systems Corporation

described under Types of Journal Content. Technical papers and CaseStudies must not exceed 30 double-spaced manuscript pages, including all figures and tables. Technical notes must not exceed 7 double-spaced manuscript pages. Papers that exceed the limits must be justified. Grossly over-length papers may be returned without review. Does this paper exceed the ASCE length limitations? If yes, please provide justification in the comments box below.	
All authors listed on the manuscript must have contributed to the study and must approve the current version of the manuscript. Are there any authors on the paper that do not meet these criteria? If the answer is yes, please explain in the comments.	No
Was this paper previously declined or withdrawn from this or another ASCE journal? If so, please provide the previous manuscript number and explain what you have changed in this current version in the comments box below. You may upload a separate response to reviewers if your comments are extensive.	No
Is this manuscript being submitted as part of a special collection? You can find active calls for papers for special collections in ASCE Journals here.	No
The flat fee for including color figures in print is $800, regardless of the number of color figures. There is no fee for online only color figures. If you decide to not print figures in color, please ensure that the color figures will also make sense when printed in black-and-white, and remove any reference to color in the text. Only one file is accepted for each figure. Do you intend to pay to include color figures in print? If yes, please indicate which figures in the comments box.	No
Is this article or parts of it already published in print or online in any language? ASCE does not review content already published with the exception of preprinted papers, thesis, and dissertations. Please review ASCE Publication Policies to ensure your	No

submission meets our criteria for submission. Please disclose details below (including DOIs, URLs, etc.) if your paper has been published in print or online previously in any format.	
Has this manuscript, in whole or in part, been submitted to a conference?	No
We require authors to disclose if Artificial Intelligence or Large Language Model tools have been used in the creation of your manuscript. Have you used any of these tools in the creation of your submission? If so, please provide detailed information below.	No
If there is anything else you wish to communicate to the editor of the journal, please do so in this box.	Dear Professor Armin W. Stuedlein, Greetings! Ms. No.- GTENG-13906R2 Thank you for your email dated July 1, 2025 regarding the decision on our manuscript to carry out minor revisions based on AE and Reviewer 1 comments to address the main issue related to the length of the manuscript. We have now made a great effort to shorten the manuscript and created Supplemental Materials (as suggested) to transfer some of the information of the main manuscript while maintaining the clarity. These changes are highlighted in the annotated version of the manuscript. Please find the re-revised version of our manuscript titled " Impact of suction and swell-induced softening on pile behavior in an unsaturated expansive clay" by Sonu Kumar, Ashutosh Kumar, Tiago Gaspar and Ashraf Osman for possible publication in the Journal of Geotechnical and Geoenvironmental Engineering as a Research paper. I would request you to process this revised manuscript at your earliest convenience. Thanking you. Warm regards Ashutosh Kumar ========== Dear Professor Armin W. Stuedlein, Greetings! Ms. No.- GTENG-13906R1 Thank you for your email dated April 7, 2025 regarding the decision on our manuscript and allowing us to revise our work. Please find the revised version of our manuscript titled (revised tittle)" Impact of suction and swell-induced softening on pile behavior in an unsaturated expansive clay" by Sonu Kumar, Ashutosh Kumar, Tiago Gaspar and Ashraf Osman for possible

	publication in the Journal of Geotechnical and Geoenvironmental Engineering as a Research paper. We have now addressed all the suggestions and concerns raised by the reviewer(s) and they are highlighted in the annotated version of the manuscript. I would request you to process this revised manuscript at your earliest convenience. Thanking you. Warm regards Ashutosh Kumar ========== Dear Professor, Please find an enclosed manuscript titled “Behaviour of single pile in unsaturated expansive clay: centrifuge testing, element testing and numerical modelling” by Sonu Kumar, Ashutosh Kumar, Tiago Gaspar and Ashraf Osman. This work is a part of the project funded through the Engineering and Physical Sciences Research Council (EPSRC) under the Global Challenges Fund programme for a project entitled ‘Developing Performance based design for foundations of wind turbines in Africa (WindAfrica) and the Commonwealth Scholarship Commission for project ‘Developing foundation guidelines for on-shore wind turbine foundation in unsaturated expansive soils’ through Split-site Scholarship. Kindly note that all the authors have contributed to the study and this manuscript is not under consideration in any other journal or conference. Please process this manuscript at your earliest convenience. Yours sincerely, Ashutosh Kumar.
ASCE is a signatory of the Sustainable Development Goals (SDG) Publishers Compact, supporting the U.N. Sustainable Development Goals listed below. You can read more about our commitment here. If your submission addresses any of these goals, please check up to five of the relevant boxes below.	**11: Sustainable Cities and Communities** - - Make cities and human settlements inclusive, safe, resilient and sustainable; **9: Industry, Innovation and Infrastructure** - - Build resilient infrastructure, promote inclusive and sustainable industrialization and foster innovation
When submitting a manuscript, authors must include a section heading titled “Data Availability Statement” before the “Acknowledgments” section or after the “Conclusion." Within the section, authors will include one or more of the following statements, as well as all citations to data, code, or models. You can read more about the Data Availability Statement policy here.	a. Some or all data, models, or code that support the findings of this study are available from the corresponding author upon reasonable request.

Please select one or more of the statements below that apply to your manuscript. The statement(s) listed in your manuscript should match those you select in your response to this question. *Note that regardless of your response to this question, all reasonable requests for data from reviewers during the review process must be fulfilled.*	
Do you intend to publish your paper under an open access license? Please note that open access papers require payment of an APC. More information about open access and fees can be found here.	No
COPYRIGHT TRANSFER AGREEMENT **I. Authorship Responsibility** To protect the integrity of authorship, only people who have significantly contributed to the research or project and manuscript preparation shall be listed as coauthors. The corresponding author attests to the fact that anyone named as a coauthor has seen the final version of the manuscript and has agreed to its submission for publication. Deceased persons who meet the criteria for coauthorship shall be included, with a footnote reporting date of death. No fictitious name shall be given as an author or coauthor. An author who submits a manuscript for publication accepts responsibility for having properly included all, and only, qualified coauthors. **II. Originality of Content** ASCE respects the copyright ownership of other publishers. ASCE requires authors	None of the exceptions listed above apply.

to obtain permission from the copyright holder to reproduce any material that (1) they did not create themselves and/or (2) has been previously published, to include the authors' own work for which copyright was transferred to an entity other than ASCE. For any figures, tables, or text blocks exceeding 100 words from a journal article or 500 words from a book, written permission from the copyright holder must be obtained and supplied with the submission. Each author has a responsibility to identify materials that require permission by including a citation in the figure or table caption or in extracted text.

More information can be found in the guide "Publishing in ASCE Journals: Manuscript Submission and Revision Requirements" (http://ascelibrary.org/doi/pdf/10.1061/9780784479018.ch05). Regardless of acceptance, no manuscript or part of a manuscript will be published by ASCE without proper verification of all necessary permissions to re-use. ASCE accepts no responsibility for verifying permissions provided by the author. Any breach of copyright will result in retraction of the published manuscript.

III. Copyright Transfer

ASCE requires that authors or their agents assign copyright to ASCE for all original content published by ASCE. The author(s) warrant(s) that the above-cited manuscript is the original work of the author(s) and has never been published in its present form.

The undersigned, with the consent of all authors, hereby transfers, to the extent

that there is copyright to be transferred, the exclusive copyright interest in the above-cited manuscript (subsequently called the “work”) in this and all subsequent editions of the work (to include closures and errata), and in derivatives, translations, or ancillaries, in English and in foreign translations, in all formats and media of expression now known or later developed, including electronic, to the American Society of Civil Engineers subject to the following:

• The undersigned author and all coauthors retain the right to revise, adapt, prepare derivative works, present orally, or distribute the work, provided that all such use is for the personal noncommercial benefit of the author(s) and is consistent with any prior contractual agreement between the undersigned and/or coauthors and their employer(s).

• No proprietary right other than copyright is claimed by ASCE.

• This agreement will be rendered null and void if (1) the manuscript is not accepted for publication by ASCE, (2) is withdrawn by the author prior to publication (online or in print), (3) ASCE Open Access is purchased by the author.

• Authors may post a PDF of the ASCE-published version of their work on their employers’ ***Intranet*** with password protection. The following statement must appear with the work: “This material may be downloaded for personal use only. Any other use requires prior permission of the American Society of Civil Engineers.”

• Authors may deposit the ***final draft*** of their work in an institutional repository or in their funding body’s designated archive upon publication in an ASCE Journal, provided the draft contains a link to the published version at ascelibrary.org, and may request public access 12 months

after publication. “Final draft” means the version submitted to ASCE after peer review and prior to copyediting or other ASCE production activities; it does not include the copyedited version, the page proof, a PDF, or full-text HTML of the published version.

• Authors may post the ***final draft*** of their work on open, unrestricted Internet sites 12 months after publication in an ASCE Journal, provided the draft contains a link to the published version at ascelibrary.org.

Exceptions to the Copyright Transfer policy exist in the following circumstances. Select the appropriate option below to indicate whether you are claiming an exception:

• U.S. GOVERNMENT EMPLOYEES: Work prepared by U.S. Government employees in their official capacities is not subject to copyright in the United States. Such authors must place their work in the public domain, meaning that it can be freely copied, republished, or redistributed. In order for the work to be placed in the public domain, ALL AUTHORS must be official U.S. Government employees. If at least one author is not a U.S. Government employee, copyright must be transferred to ASCE by that author.

• CROWN GOVERNMENT COPYRIGHT: Whereby a work is prepared by officers of the Crown Government in their official capacities, the Crown Government reserves its own copyright under national law. If ALL AUTHORS on the manuscript are Crown Government employees, copyright cannot be transferred to ASCE; however, ASCE is given the following nonexclusive rights: (1) to use, print, and/or publish in any language and any format, print and electronic, the above-

mentioned work or any part thereof, provided that the name of the author and the Crown Government affiliation is clearly indicated; (2) to grant the same rights to others to print or publish the work; and (3) to collect royalty fees. ALL AUTHORS must be official Crown Government employees in order to claim this exemption in its entirety. If at least one author is not a Crown Government employee, copyright must be transferred to ASCE by that author. • **WORK-FOR-HIRE**: Privately employed authors who have prepared works in their official capacity as employees must also transfer copyright to ASCE; however, their employer retains the rights to revise, adapt, prepare derivative works, publish, reprint, reproduce, and distribute the work provided that such use is for the promotion of its business enterprise and does not imply the endorsement of ASCE. In this instance, an authorized agent from the authors' employer must sign the form below. • **U.S. GOVERNMENT CONTRACTORS**: Work prepared by authors under a contract for the U.S. Government (e.g., U.S. Government labs) may or may not be subject to copyright transfer. Authors must refer to their contractor agreement. For works that qualify as U.S. Government works by a contractor, ASCE acknowledges that the U.S. Government retains a nonexclusive, paid-up, irrevocable, worldwide license to publish or reproduce this work for U.S. Government purposes only. This policy DOES NOT apply to work created with U.S. Government grants. as follow-up to "Do you intend to publish your paper under an open access license? Please note that open access papers require payment of an APC. More information about open access and fees can be found here."	
Please type your name below to complete the copyright transfer agreement. This will serve as your digital signature.	Ashutosh Kumar

I, the corresponding author, confirm that the authors listed on the manuscript are aware of their authorship status and qualify to be authors on the manuscript according to the guidelines above.

I, the corresponding author, confirm that the content, figures, drawings, charts, photographs, and tables in the submitted work are either original work created by the authors listed on the manuscript or work for which permission to re- use has been obtained from the creator.

I, the corresponding author, acting with consent of all authors listed on the manuscript, hereby transfer copyright or claim exemption to transfer copyright of the work as indicated above to the American Society of Civil Engineers.

as follow-up to "**COPYRIGHT TRANSFER AGREEMENT**

I. Authorship Responsibility

To protect the integrity of authorship, only people who have significantly contributed to the research or project and manuscript preparation shall be listed as coauthors. The corresponding author attests to the fact that anyone named as a coauthor has seen the final version of the manuscript and has agreed to its submission for publication. Deceased persons who meet the criteria for coauthorship shall be included, with a footnote reporting date of death. No fictitious name shall be given as an author or coauthor. An author who submits a manuscript for publication accepts responsibility for having properly

included all, and only, qualified coauthors.

II. Originality of Content

ASCE respects the copyright ownership of other publishers. ASCE requires authors to obtain permission from the copyright holder to reproduce any material that (1) they did not create themselves and/or (2) has been previously published, to include the authors' own work for which copyright was transferred to an entity other than ASCE. For any figures, tables, or text blocks exceeding 100 words from a journal article or 500 words from a book, written permission from the copyright holder must be obtained and supplied with the submission. Each author has a responsibility to identify materials that require permission by including a citation in the figure or table caption or in extracted text.

More information can be found in the guide "Publishing in ASCE Journals: Manuscript Submission and Revision Requirements" (http://ascelibrary.org/doi/pdf/10.1061/9780784479018.ch05). Regardless of acceptance, no manuscript or part of a manuscript will be published by ASCE without proper verification of all necessary permissions to re-use. ASCE accepts no responsibility for verifying permissions provided by the author. Any breach of copyright will result in retraction of the published manuscript.

III. Copyright Transfer

ASCE requires that authors or their agents assign copyright to ASCE for all

original content published by ASCE. The author(s) warrant(s) that the above-cited manuscript is the original work of the author(s) and has never been published in its present form.

The undersigned, with the consent of all authors, hereby transfers, to the extent that there is copyright to be transferred, the exclusive copyright interest in the above-cited manuscript (subsequently called the “work”) in this and all subsequent editions of the work (to include closures and errata), and in derivatives, translations, or ancillaries, in English and in foreign translations, in all formats and media of expression now known or later developed, including electronic, to the American Society of Civil Engineers subject to the following:

• The undersigned author and all coauthors retain the right to revise, adapt, prepare derivative works, present orally, or distribute the work, provided that all such use is for the personal noncommercial benefit of the author(s) and is consistent with any prior contractual agreement between the undersigned and/or coauthors and their employer(s).

• No proprietary right other than copyright is claimed by ASCE.

• This agreement will be rendered null and void if (1) the manuscript is not accepted for publication by ASCE, (2) is withdrawn by the author prior to publication (online or in print), (3) ASCE Open Access is purchased by the author.

• Authors may post a PDF of the ASCE-published version of their work on their employers’ *Intranet* with password protection. The following statement must appear with the work: “This material may be downloaded for personal use only. Any

other use requires prior permission of the American Society of Civil Engineers."

• Authors may deposit the ***final draft*** of their work in an institutional repository or in their funding body's designated archive upon publication in an ASCE Journal, provided the draft contains a link to the published version at ascelibrary.org, and may request public access 12 months after publication. "Final draft" means the version submitted to ASCE after peer review and prior to copyediting or other ASCE production activities; it does not include the copyedited version, the page proof, a PDF, or full-text HTML of the published version.

• Authors may post the ***final draft*** of their work on open, unrestricted Internet sites 12 months after publication in an ASCE Journal, provided the draft contains a link to the published version at ascelibrary.org.

Exceptions to the Copyright Transfer policy exist in the following circumstances. Select the appropriate option below to indicate whether you are claiming an exception:

• U.S. GOVERNMENT EMPLOYEES: Work prepared by U.S. Government employees in their official capacities is not subject to copyright in the United States. Such authors must place their work in the public domain, meaning that it can be freely copied, republished, or redistributed. In order for the work to be placed in the public domain, ALL AUTHORS must be official U.S. Government employees. If at least one author is not a U.S. Government employee, copyright must be transferred to ASCE by that author.

• CROWN GOVERNMENT COPYRIGHT: Whereby a work is prepared by officers of

the Crown Government in their official capacities, the Crown Government reserves its own copyright under national law. If ALL AUTHORS on the manuscript are Crown Government employees, copyright cannot be transferred to ASCE; however, ASCE is given the following nonexclusive rights: (1) to use, print, and/or publish in any language and any format, print and electronic, the above-mentioned work or any part thereof, provided that the name of the author and the Crown Government affiliation is clearly indicated; (2) to grant the same rights to others to print or publish the work; and (3) to collect royalty fees. ALL AUTHORS must be official Crown Government employees in order to claim this exemption in its entirety. If at least one author is not a Crown Government employee, copyright must be transferred to ASCE by that author.

• WORK-FOR-HIRE: Privately employed authors who have prepared works in their official capacity as employees must also transfer copyright to ASCE; however, their employer retains the rights to revise, adapt, prepare derivative works, publish, reprint, reproduce, and distribute the work provided that such use is for the promotion of its business enterprise and does not imply the endorsement of ASCE. In this instance, an authorized agent from the authors' employer must sign the form below.

• U.S. GOVERNMENT CONTRACTORS: Work prepared by authors under a contract for the U.S. Government (e.g., U.S. Government labs) may or may not be subject to copyright transfer. Authors must refer to their contractor agreement. For works that qualify as U.S. Government works by a contractor, ASCE acknowledges that the U.S. Government retains a nonexclusive, paid-up, irrevocable, worldwide license to publish or reproduce this work for U.S. Government purposes only. This policy DOES NOT apply to work created with U.S. Government grants.

"	

Powered by Editorial Manager® and ProduXion Manager® from Aries Systems Corporation

Cover Letter Click here to access/download;Cover Letter;Cover_letter.docx

From
Dr. Ashutosh Kumar.
Assistant Professor,
School of Civil and Environmental Engineering, IIT Mandi
Mandi, Postcode- 175005.
Visiting Fellow, Institute of Hazard, Risk and Reslience,
Durham University, United Kingdom.
Email: ashutosh@iitmandi.ac.in

Date: July 15, 2025

To
Professor Armin W. Stuedlein,
Journal of Geotechnical and Geoenvironmental Engineering.

Sub: Submission of a Re-Revised Manuscript for possible publication in Geotechnical and Geoenvironmental Engineering. (Ms. No. GTENG-13906R2)

Dear Professor,

Thank you for your email dated July 1, 2025 regarding the decision on our manuscript and allowing us to revise our work based on AE and Reviewer 1 minor comments. Please find the re-revised version of our manuscript titled “Impact of suction and swell-induced softening on pile behavior in an unsaturated expansive clay" by Sonu Kumar, Ashutosh Kumar, Tiago Gaspar and Ashraf Osman for possible publication in the Journal of Geotechnical and Geoenvironmental Engineering as a Research paper.

We have now addressed all the suggestions and concerns raised by Reviewer 1 and the AE and they are highlighted in the annotated version of the manuscript.

I would request you to process this revised manuscript at your earliest convenience.

Thanking you.
Warm regards
Ashutosh Kumar

Manuscript
Click here to access/download;Manuscript;Manuscript-GTENG-13906R2.docx

Name of Journal: *Journal of Geotechnical and Geoenvironmental Engineering*

Article Type: Technical paper

Date of Re-Revised Submission: 15.07.2025

Number of words, figures and tables: 7791, 12, 4

Impact of suction and swell-induced softening on pile behavior in an unsaturated expansive clay

Sonu Kumar[1], Ashutosh Kumar[2*], Tiago A.V. Gaspar[3] and Ashraf S. Osman[4]

Author 1

Sonu Kumar, M.Tech., Ph.D. Research Scholar, School of Civil and Environmental Engineering, Indian Institute of Technology Mandi, IIT Mandi, 175005, India. Commonwealth Scholar, Durham University, DH1 3LE, United Kingdom. Email: d20015@students.iitmandi.ac.in

Author 2

[*]Ashutosh Kumar, Ph.D., Assistant Professor, School of Civil and Environmental Engineering, Indian Institute of Technology Mandi, IIT Mandi, 175005, India. Visiting Fellow, Institute of Hazard, Risk and Resilience, Durham University, United Kingdom. Email: ashutosh@iitmandi.ac.in ([*]Corresponding author)

Author 3

Tiago A.V. Gaspar, Ph.D., Lecturer, Department of Civil and Environmental Engineering, Imperial College London, SW7 2AZ, United Kingdom. Email: t.gaspar@imperial.ac.uk

Author 4

Ashraf S. Osman, Ph.D., Professor, Department of Engineering, Durham University, DH1 3LE, United Kingdom. Email: ashraf.osman@durham.ac.uk

Abstract

The study examines the response of a single pile embedded in an unsaturated expansive clay. This was achieved by performing three-dimensional finite element analyses, employing the Barcelona Basic Model. The study aimed to quantify the contribution of suction and swell-induced softening in dictating the mobilization of shaft resistance. Centrifuge testing was used as a benchmarking study to simulate the free swell and pile pull-out response. The resulting coupled hydro-mechanical flow deformation analyses effectively captured swell evolution, changes in lateral swell pressure and swell-induced softening, all of which significantly influenced load mobilization along the pile length. The results obtained identified zones of both positive and negative shaft resistance along the pile, previously overlooked by studies focusing solely on the development of positive resistance within the active zone. The development of tensile load in the pile was closely correlated with the reduction in suction and resulting swell upon wetting. During initial wetting, reduction of suction to the air occlusion value (where only 18% of total swell had been achieved) produced the maximum tensile load, after which reductions were observed. Furthermore, in comparison to rainfall infiltration, a rise in the water table was found to be a more critical hydraulic condition, generating maximum axial load and pile uplift. The study also highlighted conservatism in calculating pile capacity based on saturated soil mechanics, with the capacity found to be around five times lower than under unsaturated conditions. These findings enhance the understanding of pile foundation design in unsaturated expansive clays.

Keywords: Pile foundation; Expansive soils; Unsaturated soils; Suction; Centrifuge testing; Finite element modeling.

Introduction

Expansive soils exist worldwide, often remaining unsaturated where evapotranspiration surpasses precipitation, and can extend to depths ranging from 7 to 30 meters (Elsharief 2012; Byrne et al. 2019). Further, seasonal fluctuations in water content to considerable depths cause certain soil profiles to undergo swelling and shrinkage (Gens 2010). This behavior is typical of soils having active clay minerals such as smectite, which interact with water at the microstructural level significantly influencing their macrostructural response (Gens and Alonso 1992; Al-Dakheeli and Bulut 2019). Soil swell or shrink often results in serviceability issues such as foundation uplift or settlement (Jennings and Kerrich 1962; Chen 1975; Li et al. 2014). To address these challenges, pile foundations are commonly employed where piles penetrate through the active zone (depth prone to volume change) and transfer the superstructure load to more stable and deeper soil layers.

The estimation of shaft resistance within the active zone has historically been based on simplified assumptions, such as assuming a linear swell profile with depth and using total or effective stress-based methods (Terzaghi 1925; Poulos 1989; Challa and Poulos 1991; Benvenga 2005; Nelson et al. 2012). Closed-form elastic solutions and numerical methods have also been proposed while treating swell as an external displacement boundary condition (Fan et al. 2007; Xiao et al. 2011; Jiang et al. 2020). da Silva Burke et al. (2022) summarized these methods and proposed modifications to the conventional elastic solutions. Several studies have highlighted the role of soil suction in dictating the shaft resistance of piles (Liu and Vanapalli 2019; Liu and Vanapalli 2022; Wu and Vanapalli 2022; Kumar and Kumar 2023). These studies proposed analytical and numerical solutions based on unsaturated soil mechanics principles assuming elastic behavior for the expansive clay. Additionally, the selection of elastic parameters at various suction levels is based upon empirical relations which are mostly suitable at small strains and tend to overestimate the shaft resistance at large strains (da Silva

Burke et al. 2022). Therefore, shaft resistance at large strains is commonly capped at a limiting value to prevent overestimation of tensile axial loads, though establishing this limit generally requires interface shear strength parameters or field-testing results. Numerically, the post-peak reduction in shaft resistance can be reasonably captured by implementing relative pile-soil slip conditions or using strain-softening interface models (Poulos 1989; Pham et al. 2024).

Fundamentally, the pile-soil-swell mechanism is governed by complex interactions of competing mechanisms at the pile-soil interface, as shown in Fig. 1. Initially, with swell evolution, lateral confinement at the pile-soil interface increases as lateral swell pressure develops (Abdollahi and Vahedifard 2021) leading to an increase in shaft resistance (Blight 1984). Thereafter, the loss of suction and macrostructural realignment within the soil begins to dominate soil behavior resulting in swell-induced softening (Gens and Alonso 1992), which subsequently reduces pile shaft resistance (Elsharief et al. 2007; Smit et al. 2019; Gaspar et al. 2024).

The presence of a stable zone simplifies the problem by providing an anchorage in the lower part of the pile length, allowing an increase in positive shaft resistance in the active zone to be balanced by a corresponding increase in the negative shaft resistance in the stable zone. The depth of the active zone in the field varies and in extreme cases may exceed the embedded length of the pile. Therefore, the performance of the pile foundation needs to be thoroughly assessed, necessitating a comprehensive investigation. Nevertheless, there is a lack of detailed studies in the literature that properly quantify the pile-soil-swell mechanism in the active zone. This study investigates the mechanical behavior of a single pile embedded in an unsaturated expansive clay subjected to wetting-induced swelling. This was achieved by performing three-dimensional finite element (3D-FE) numerical modeling incorporating the Barcelona Basic Model. Centrifuge testing was used as a benchmarking study to first understand the evolution of swell and quantify the loss of shaft resistance during pile pull-out testing. The numerical

analysis: (a) validated the centrifuge test results (b) investigated the response of a free-standing pile subjected to hydraulic loading and (c) explored pile response under combined hydraulic and mechanical loading. The main aim of this study was to quantify the effects of suction loss, lateral swell pressure and swell-induced softening on pile-soil-swell mechanisms under varied degrees of swelling, thereby overcoming the limitations of the benchmarking centrifuge study.

Centrifuge Testing as Benchmarking Study

The centrifuge tests considered simulated an expansive clay (liquid limit = 92% and plasticity index = 55%) profile targeting an average dry density of 1350 kg/m³ and water content of approximately 31% based on site data from a bentonite mine located 350 km northeast of Pretoria, in the Limpopo province of South Africa (Gaspar et al. 2024). The tests were performed using the geotechnical centrifuge facility at the University of Pretoria (Jacobsz et al. 2014). This study used centrifugal acceleration of 30g to achieve appropriate prototype stresses, scaled to replicate expansive clay profiles typical of many South African regions. Further details on centrifuge model preparation are available in Smit et al. (2019) and Gaspar et al. (2023); a summary is provided here, with all dimensions given at model scale unless otherwise stated.

The clay profile within the centrifuge strongbox was carefully prepared to mimic the in-situ fissured structure of expansive clays. Intact clay lumps were collected at their natural water content, grated and statically compacted into a 50 mm high mold (under K_o conditions) to match the in-situ average dry density. Once compacted, the resulting clay slabs were trimmed to final dimensions of 335 mm × 152 mm × 50 mm and placed in the centrifuge strongbox. The final clay profiles consisted of several clay slabs, separated by needle-punched non-woven geotextile layers to enable rapid water ingress. The slabs were confined between two perforated geotextile-covered steel plates with water wells on either side. This allowed for three-dimensional infiltration where water ingress happened from the bottom, sides and top of each

clay slab. Within the centrifuge model, time for infiltration into the fissured clay is initially governed by the scaling law for seepage velocity (scaling factor N). After the closure of fissures, the rate of water infiltration (and thus the swell process) is dictated by a diffusive scaling law (scaling factor N^2) as reported by Caicedo et al. (2006) and Gaspar et al. (2023). The fissured clay structure together with the inclusion of geotextiles, enabled rapid water migration and reduced suction, allowing the target swell to be achieved in a reasonable time.

Fig. 2 presents a schematic diagram of the centrifuge setup. The details of the centrifuge model having dimensions of 335 mm × 152 mm × 250 mm aimed at modeling the free swell mechanism (greenfield conditions) is given in Fig. 2(a). The swell in this model was monitored at the top of each clay slab using extensometers whereas surface swell was monitored using three separate linear variable differential transformers (LVDTs) placed on the surface of the top slab. Volumetric water content and matric suction were monitored using volumetric moisture content sensors (5TM probe by Meter Group 2017a) and fixed-matrix porous ceramic sensors (Teros 21 sensor by Meter Group 2017b) respectively. Fig. 2(b) provides the details of the centrifuge model having dimensions of 335 mm × 152 mm × 200 mm aimed at investigating the change in shaft resistance along the pile length for unswelled and targeted swell states (swell equal to 2.5%) as proposed by Van der Merwe (1964) for a clay of "very high potential expansiveness".

Four bored piles were installed at 1g into the clay profile (average dry density = 1350 kg/m^3 and degree of saturation = 93%) by augering 20 mm diameter holes to a depth of 180 mm and filling the holes with a rapid hardening grout. A 4 mm diameter, stainless steel threaded rod was cast concentrically within each pile to simulate steel reinforcement, and the grout was left to cure for a period of 14 hours before testing. The model piles were designed to represent a full-scale 600 mm diameter reinforced-concrete pile with 6 x 20 mm diameter longitudinal

reinforcing bars (for more details see Gaspar (2020) and Louw et al. (2022)). The material properties of the grout are summarized in Table 1.

While the measured compressive and tensile strengths are consistent with typical structural concrete, the Young's modulus of the grout is comparatively low. To compensate for this, a somewhat higher volume of reinforcement (4% by cross-sectional area) was employed to achieve an axial stiffness (*EA*) representative of the prototype pile. The center to center spacing of the piles was 3.35 times (clear spacing of 2.35 times) the pile diameter while the spacing of the edge piles from the perforated steel plates was maintained at 2.85 times the pile diameter, sufficient to avoid any boundary effects during pile pull-out (Song 2008; Panchal and McNamara 2018; Lalicata et al. 2023; Lalicata et al. 2024). No moisture or suction sensors were installed in this test due to limited space.

The centrifuge testing successfully captured the swell evolution (targeted and final surface swell of 2.5% and 6% in 14 h and 110 h respectively), effect of overburden pressure in limiting swell at depths and swell-induced softening on the pile pull-out resistance (a reduction of around 50% in peak shaft friction between unswelled and targeted swell conditions). The detailed discussion on the results is reported in following section.

Insights from free-swell centrifuge testing revealed that measuring water content and suction in fissured soils can be unreliable, as rapid moisture ingress along fissures leads to readings that do not reflect the behavior of the bulk soil mass (Gaspar et al. 2023). Consequently, no measurements of suction or volumetric water content were obtained during swelling. To address this limitation, numerical modeling was employed to investigate the pile–soil–swell mechanism and understand the role of suction in controlling the pile response under varying swell conditions.

Numerical Modeling

The mechanical behavior of the unsaturated expansive clay was modeled using the critical state-based Barcelona Basic Model (BBM), available in the standard PLAXIS library (Alonso et al. 1990; PLAXIS 2023a). In PLAXIS, the model is implemented with Bishop's stress and suction as independent stress variables. For the pile material, a non-porous linear elastic constitutive model was used, characterized by a modulus of elasticity of 11.9×10^6 kN/m² and Poisson's ratio of 0.2. These values indicate that the pile material exhibits linear elastic behavior within the range of applied loads and its axial load response is primarily governed by shaft friction changes (Lalicata et al. 2023). The pile-soil interface behavior follows a stress-dependent elastoplastic interface model, as provided in PLAXIS (PLAXIS 2023b).

The 3D-FE models were developed at prototype-scale dimensions, using a length scaling factor of $N = 30$ applied to the dimensions of the centrifuge model as shown in Fig. 3. This modeling approach was adopted to mimic the three-dimensional ingress of water into the clay (Bilotta and Stallebrass 2009; Soranzo et al. 2015; Lalicata et al. 2022; Wu and Vanapalli 2022). Fig. 3(a) shows a 3D-FE model measuring 10 m in length, 4.56 m in width and 7.5 m in height developed to mimic the conditions of free swell in centrifuge testing, presented in Fig. 2(a). Fig. 3(b) shows a 3D-FE model measuring 10 m in length, 4.56 m in width and 6 m in height developed to simulate the pile pull-out response in centrifuge testing, presented in Fig. 2(b). Utilising symmetry, two single piles each having a length of 5.4 m and diameter of 0.6 m,spaced at a clear distance of 5.7 times of pile diameter were modeled as wished-in-place using volumetric elements. The contact between the pile and the soil was discretized using the standard interface elements with specific mesh refinement at the pile-soil interface. The 3D-FE model mesh consists of 338823 (Fig 3(a)) and 343286 (Fig. 3(b)) 10-noded tetrahedral elements adopted after a mesh sensitivity study.

Boundary Conditions

The displacement boundaries were constrained normally on all sides and fully restrained at the bottom, while the top surface remained free (Fig. 3(a)&(b)). The pull-out displacement was applied normally at the pile head as a mechanical boundary condition. To address potential detachment during pull-out causing numerical instability, a very low axial stiffness was applied at the pile base and adjacent soil surface boundary. To mimic wetting during centrifuge testing, the hydraulic boundaries in the 3D-FE models at the sides, top, bottom and within each model were defined and kept open to allow three-dimensional water ingress into the clay layers. Starting at the bottom of the models, water level rise and infiltration through geotextile layers were simulated by applying zero pore-pressure condition along the boundaries of each clay slab, over a duration of 900 mins. Such a condition represented the rapid reduction in suction along the outermost portions of the clay slabs and the geotextile layers (given their comparably higher permeability). The timeframe of 900 mins mimicked the centrifuge seepage time, following the relevant scaling law for seepage velocity. The imposition of the zero pore-pressure condition was incrementally applied along the relevant boundaries of the model, thereby simulating the rising water surface in the corresponding centrifuge model. Once the water surface had reached its final position above the surface of the clay profile, swell was allowed to occur for a period of 4125 days. This timeframe mimicked the centrifuge swell progression, following the scaling law for diffusive processes. Table 2 lists the sequence of hydraulic loading applied during centrifuge testing and numerical modeling.

Initial Conditions and Analysis Methodology

The 3D-FE models were developed at an initial average dry density and gravimetric water content of the clay slabs used in construction of the soil profile during centrifuge testing. This helped in estimation of initial void ratio (e_0 = 0.94), saturated unit weight (γ_{sat} = 18.45 kN/m^3), bulk unit weight (γ_b = 17.85 kN/m^3) and initial degree of saturation (S_r = 93%). A uniform

initial suction of 804 kPa was applied to the soil model, derived from the soil water retention curve (SWRC) corresponding to S_r = 93%, (as detailed in following section). It should be noted that the choice of initial void ratio directly influences the magnitude of swell (Gaspar et al. 2022).

The initialization of effective stresses was performed using the K_o procedure (Jaky 1944; Conti et al. 2014; Soranzo et al. 2015; PLAXIS 2023c). This methodology was adopted since the clay slabs used for centrifuge testing were prepared under K_o conditions and remained under K_o conditions throughout testing due to the lateral confinement offered within the centrifuge strongbox. Furthermore, since model piles prevented lateral straining for adjacent clay, this assumption of stress state is also valid for the simulated pile pull-out tests, particularly for soil elements closest to the pile shaft.

The piles were then activated by assigning the material density to the volume occupied by the pile, along with the activation of interface elements. Since the piles were modeled as wished-in-place, drained effective stress-based plasticity analysis was used during their activation phase. The pile pull-out response at unswelled and targeted swell states was simulated using fully coupled flow deformation analysis scheme (Galavi 2010). This scheme was further employed to simulate the swelling of the soil, achieved through the incremental loss of suction throughout the clay profile. The analysis sequence followed during centrifuge testing and 3D-FE modeling is summarized in Table 2.

Element Scale Testing and BBM Parameters Calibration

Constitutive Model Parameters

The constitutive parameters for the South African clay were determined through element-scale laboratory testing. The sample preparation technique mimicked the natural “fissured structure” with soil being grated and compacted to match in-situ conditions. The consolidated undrained (CU) triaxial testing performed on the saturated samples was used to calibrate the saturated

state BBM parameters. Single-element numerical simulations were carried out using the PLAXIS SoilTest module. To model the saturated soil behavior, the BBM requires the critical state friction angle ϕ'_{cr}, the slope of normal compression line λ in υ (specific volume) : ln p' space, the slope of swelling line κ in υ : ln p' space and Poisson's ratio ν'. For the initialization of the yield surface, parameters such as reference effective pressure p'_r, initial void ratio e_o and OCR are also needed. The goal was to identify a single set of saturated state BBM parameters that provided the best overall fit for the tests conducted. The details on the calibration procedure are provided in Appendix S1. It should be noted that the BBM parameters, calibrated against element test results, captured the observed behavior with reasonable accuracy, thereby implicitly accounting for the fissured nature of the clay.

For modeling the unsaturated soil response, the BBM requires the following parameters which describe: the elastic response with change in suction governed by the slope of the swelling line κ_s (υ : ln s space), the increase in apparent cohesion with suction dictated by parameter k_s, changes in soil stiffness with suction controlled by parameter r, and the rate of increase in soil stiffness with suction controlled by parameter β. Identifications of these parameters from experimental data are shown in Appendix S2.

Soil Water Retention Curve

The soil-water retention curve (SWRC) was determined using a modified contact filter paper method, with slight deviation from the procedure outlined in ASTM (2010) to account for challenges in preparing high-plasticity clay samples at high initial saturation. Measurements for a drying curve were taken on initially saturated oedometer samples (75 mm in diameter) following loading and unloading phases. Two Whatman Grade 42 filter papers were placed on one side of each sample, which was wrapped in clingfilm and sealed for 7 days to allow suction equilibration after each drying phase. Importantly, during equilibration the sample was placed such that the side with the filter paper was facing downwards, with a 100 g mass placed on top

276 of the sample to ensure good contact between filter paper and soil. The volume of the sample
277 was measured using a digital vernier caliper (±0.01 mm resolution), and the SWRC was plotted
278 in terms of degree of saturation S_r and suction head ψ, as shown in Fig. 4(a).
279 Contact suction measurements on low-permeability soils can overestimate internal suction due
280 to the higher drying of surface layers, especially in samples with high surface area-to-volume
281 ratios (Esmaili and Hatami 2017; Azizi et al. 2020). This was evident from suction
282 measurements presented by Gaspar et al. (2023), where a suction of 1200 kPa (S_r = 87%) was
283 measured inside the clay slab using a fixed-matrix porous sensor. In contrast, suction estimated
284 from the SWRC measured using the contact filter paper method (on significantly smaller
285 samples) produced a suction of 13.45 MPa. Hence to better represent SWRC of larger soil
286 volumes, a lateral shift in the SWRC was implemented, following the approach outlined by
287 Fredlund et al. (2011) by adjusting the fitting parameter related to the air entry value g_a, while
288 ensuring congruity between the original and shifted data by keeping g_n unchanged, which is a
289 parameter related to the rate of water extraction/imbibition (Fig. 4(a)). This shift was done such
290 that the SWRC measured using the filter paper method, corresponded with the measured matric
291 suction within the centrifuge model using fixed –matrix porous sensors. Moreover, the SWRC
292 of the soil tested herein did not show any significant hysteresis in the range of suction
293 measurement of interest (Gaspar 2020); therefore, the primary drying SWRC was used to
294 simulate swelling during wetting.
295 The hydro-mechanical model parameters were obtained by using the van Genuchten model
296 (VG model) to fit a curve through shifted SWRC (van Genuchten 1980) as shown in Fig. 4(a).
297 The curve fitting was carried out where initial degree of saturation S_{inl} = 96.5% was calculated
298 from measurements on the oedometer sample at the end of oedometer testing. The residual
299 degree of saturation S_{res} = 30% was obtained after prolonged drying of the soil sample under

ambient conditions in a controlled temperature room (22 ºC ± 1 ºC) followed by a drying in a desiccator chamber until no change in moisture content for 2 weeks was recorded.

Further, within the numerical scheme the coefficient of saturated hydraulic conductivity k_{sat} was updated with changes in void ratio e using the permeability index c_k following the expression $k_{sat} = k_{sat,input} \times 10^{(e-eo)/ck}$ (Tavenas et al. 1983). The input parameters $k_{sat,input}$ at the initial void ratio e_o and c_k (slope of line in k_{sat} : e space) were determined from an oedometer test conducted on a reconstituted sample, as reported by Gaspar et al. (2022). Using the results of this test, the k_{sat} with changing void ratio was calculated using Terzaghi's consolidation theory, as shown in Fig. 4(b). It should be noted that in fissured clay, the initial hydraulic conductivity may significantly exceed k_{sat} due to open fissures. However, during a swell process, this higher hydraulic conductivity is only momentarily applicable as swelling rapidly closes fissures, causing conductivity to drop sharply by several orders of magnitude to much lower unsaturated levels (k_{unsat}). With continued wetting, increased void ratio and reduced suction gradually raise k_{unsat}. Due to the high variability in hydraulic conductivity throughout swell, k_{sat} was chosen as a representative intermediate value, an approach validated by the accurate simulation of swelling over time in the 3D-FE model in comparison to centrifuge test (see next section).

The standard interface model available in PLAXIS library was used for simulating the soil–structure interaction response. The details on interface model parameters are provided in Appendix S3. All the BBM and interface model parameters are summarized in Table 3.

Results

This section compared the results of centrifuge testing and numerical modeling for free swell and pile pull-out testing performed at unswelled and targeted swell conditions.

Free Swell

Fig. 5(a) shows the progression of surface swell over time, along with the corresponding suction reduction. Herein, suction represents an 'average suction' as determined by averaging the values at the centre of each clay slab. The imposed hydraulic boundaries advanced the wetting front within the soil, increasing the degree of saturation and leading to a non-linear decrease in suction with time from 804 kPa to residual value of nearly zero. The swell evolution follows a non-linear variation with time. The 3D-FE model accurately predicted surface swell over 4125 days, exhibiting a final surface swell Δh_f = 6%. Firstly, suction reduction near to an air occlusion value (AOV) of 200 kPa resulted in a surface swell Δh = 1.8% within 250 days (approximately one-third of Δh_f). Subsequently, when suction reduced from the AOV to residual level, an additional 4.2% of the swell was observed, though at a decreasing rate. Notably, the initial larger suction loss of 600 kPa caused less swelling compared to the later 200 kPa loss because initial high suction in expansive clays (which includes significant capillary forces) tightly binds the soil particles, restricting their movement and limiting swelling. As matric suction decreases, these forces weaken, allowing the soil to expand more freely (Tripathy et al. 2002; Lloret et al. 2003).

Fig. 5(b) shows the variation of swelling with normalized depth, where normalization was done using total soil depth. At the surface, swell can be seen to occur relatively freely, however, at deeper depths the effect of overburden pressure led to a reduction in swelling. The targeted surface swell of 2.5% (6.25 mm) was achieved in 525 days where the average suction had dropped to 102 kPa, significantly below the AOV. The 3D-FE model reasonably captured the nonlinear variation of swelling with depth as observed during centrifuge testing.

Pile Pull-out

Fig. 6 shows the evolution of swell and its impact on the development of pile shaft capacity using pile pull-out testing. Closely comparable to centrifuge testing, a targeted surface swell of

2.5% (5 mm) was achieved within 375 days in 3D-FE model (Fig. 6(a)). During this period, the average suction in the soil profile dropped from an initial value of 804 kPa to 130 kPa, well below the AOV. Such a dramatic reduction in suction provides a preliminary indication for the potential for swell-induced softening. Fig. 6(b) shows the mobilized shaft friction with normalized pile displacement δ_{ps} (normalized using pile diameter d) comparing the unswelled and targeted swell conditions. The impact of swell-induced softening is evident as the pile pull-out test conducted after achieving the targeted surface swell, illustrated an approximately 50% decrease in peak shaft friction. However, at the unswelled state, the 3D-FE model results were slightly conservative, showing a difference of 15 kPa in peak shaft friction compared to the centrifuge tests. Nonetheless, these results closely captured the initial slope (vital for serviceability considerations) and peak shaft friction response.

It is important to note that while the numerical simulations effectively captured the impact of swell-induced softening on peak shaft friction, they did not fully replicate the strain-softening behavior observed during the pile pull-out test under unswelled conditions. This limitation primarily arises from the inability of the selected constitutive model to accurately simulate strain softening at the pile–soil interface (Pham et al. 2024). Despite this, the numerical model accurately predicted the behavior of the test conducted at the targeted swell magnitude, where yielding was observed at a normalized displacement of approximately 6.5% and remained at this plateau while shearing progressed. Therefore, it can be stated that the chosen numerical model was able to validate the swell mechanism and resulting response of pile behavior both qualitatively and quantitatively. However, caution is required in interpretating results where strain softening is expected, as is the case at higher suction levels (in this study, at s = 804 kPa). The proposed numerical model is further extended to perform the parametric study as presented in the following section.

Parametric Study

After ascertaining the accuracy of the 3D-FE model, a parametric study was conducted to investigate the pile-soil-swell mechanism. Three different cases were considered to study the behavior of a single pile (length 6.5 m and diameter 0.6 m) under varied magnitudes of swell. Case 1 is a free-standing single pile under the same hydraulic loading condition of internal drains simulated in centrifuge testing; Case 2 is a free-standing single pile subjected to different hydraulic loading conditions; and Case 3 is a combined scenario where the pile was loaded in compression and subjected to hydraulic loading. Herein, the free-standing pile refers to a pile foundation carrying no mechanical loading. A pile subjected to compressive load refers to a pile foundation carrying the external load placed at pile head. Additionally, the hydraulic boundary applied at the soil base and top surface were employed to simulate rising water table (RWT) and rainfall infiltration (RI) respectively, representing real-case water conditions encountered in the field.

Case 1: Free-standing Pile

Fig. 7 shows the change in mechanical behavior of a free-standing pile, subjected to varied degrees of surface swell ($\Delta h/\Delta h_f$) where Δh and Δh_f are the surface swell at a given instant and final swell, respectively. Fig. 7(a) shows the variation of normalized pile-soil relative displacement δ_{ps} with pile length L. The δ_{ps} was calculated at pile-soil interface by subtracting the displacement of the pile from the soil displacement and normalized with respect to the pile diameter d. The results show that both positive and negative δ_{ps} increased with an increase in the magnitude of swell, causing the formation of a neutral plane around the mid-length of the pile. In the zone above the neutral plane, soil swell exceeds pile uplift, while below the neutral plane, the reverse occurs, however, it is important to note that this transition occurs within the active zone. This observation was also highlighted by da Silva Burke et al. (2022) in the

399 analysis of large-scale field testing, whereas previous studies had assumed a positive δ_{ps}
400 throughout the active zone (Fan et al. 2007; Xiao et al. 2011; Jiang et al. 2020).
401 From Fig. 7(a), it can also be seen that the downward movement of neutral plane is relatively
402 modest, starting from 3.2 m from the pile top and ending at 3.6 m for $\Delta h/\Delta h_f$ of 0.1 and 1.0
403 respectively. This impacted the mobilization of shaft friction along the pile length (Fig. 7(b)).
404 Above the neutral plane, positive δ_{ps} leads to the development of positive shaft friction, creating
405 a pile pull-out effect. Conversely, below the neutral plane, negative δ_{ps} results in negative shaft
406 friction, generating a pile anchoring effect (negative skin friction). It is important to highlight
407 that the pile experienced a limiting shaft friction of 80 kPa in the 3D-FE model. This value
408 compared well with calculated value of limiting shaft resistance obtained using the Eslami and
409 Fellenius (1997) approach, where an average shaft correlation coefficient C_s of 1.75% was
410 multiplied with the average cone penetration resistance data reported by Gaspar et al. (2023),
411 yielding a limiting shaft friction of 78 kPa (see da Silva Burke et al. (2022) for additional details
412 for estimation of limiting shaft friction).
413 Notably, the mobilization of limiting shaft friction in 3D-FE both in positive and negative
414 directions occur early at $\Delta h/\Delta h_f = 0.10$. The limiting shaft friction begins near the pile head and
415 the pile base (approximately within $L/3$ on either side), which is likely due to the greater
416 shearing caused by higher δ_{ps} (Fig. 7(a)). This 'pre-loading' that occurs during the swell process
417 results in a reduction in reserve tensile capacity, which can be critical in engineering projects
418 involving lightly loaded or incomplete structures, laterally loaded or tensile piles. In such cases,
419 if the pile foundation is not adequately designed to resist the additional swell-induced tensile
420 forces, this condition may lead to cracking or structural damage of the pile elements.
421 The further increment in swelling from $\Delta h/\Delta h_f = 0.10$ to $\Delta h/\Delta h_f = 1$ caused dramatic reduction
422 in shaft resistance (from 80-10 kPa) despite increasing values of δ_{ps}. This is attributed to the
423 dominant effect of suction at lower swell magnitude (s = 740 kPa at $\Delta h/\Delta h_f = 0.10$) which

provided significantly higher shear strength. In contrast, the effect of large reductions in suction accompanied by swell-induced softening at $\Delta h/\Delta h_f$ = 1, resulted in reduced mobilized shaft friction. Moreover, while approaching $\Delta h/\Delta h_f$ = 1, the overburden effects became more significant, resulting in greater negative shaft friction (20 kPa) compared to positive shaft friction (10 kPa), causing the neutral plane to shift downward.

The opposing positive and negative shaft friction during swelling led to the development of tensile axial load in the pile, as shown in Fig. 7(c). The location of the maximum tensile axial load was aligned with the position of the neutral plane. However, counterintuitively, the maximum tensile axial load did not occur at the onset of limiting shaft friction at a swell level of $\Delta h/\Delta h_f$ = 0.10, but rather at $\Delta h/\Delta h_f$ = 0.18.

Fig. 8 illustrates the variation of maximum tensile axial load and its dependence on both suction and lateral swell pressure. In Fig. 8(a), the maximum tensile axial load, normalized by the pile uplift capacity P_{ult} is shown at different degrees of swell $\Delta h/\Delta h_f$. The normalized variation in suction is also plotted, using the initial suction value (804 kPa) as a normalizing factor. The pile uplift capacity P_{ult} of 75 kN was calculated using the β method (Chandler 1968; Burland 1973) expressed by $P_{ult} = K_o\sigma'_v\tan\phi'(\pi dL)$. In the above formulation, d is the pile diameter, L is the pile length and ϕ' is assumed equal to ϕ'_{cr}. The vertical effective stress (σ'_v) was calculated at the centre of pile assuming saturated conditions. The lateral earth pressure coefficient K_o was estimated using K_o = 1 - $\sin\phi'_{cr}$ (Jaky 1944) as a simplification to provide a lower-bound estimate of horizontal stress in saturated conditions. Initially, the free-standing pile was under compression due to self-weight, as swelling progresses, shearing at the pile–soil interface mobilizes positive shaft resistance which was counteracted by emerging negative resistance thereby inducing tensile loads in the pile. Driven by lateral confinement and high suction, the tensile load rises sharply, peaking at about 5.18 times the ultimate capacity (P_{ult}) at $\Delta h/\Delta h_f$ = 0.18 (around 500 kPa suction). Beyond $\Delta h/\Delta h_f$ > 0.20, suction loss and macrostructural

adjustments trigger swell-induced softening, leading to a reduction in positive shaft resistance and a gradual decrease in tensile axial load.

Fig. 8(b) shows the evolution of the stress path for soil elements (U1, U2 and U3) located along the pile length. The K_o and K_p (passive earth pressure coefficient) lines are also included for comparison (Rotisciani et al. 2017). The K_p corresponds to the maximum lateral pressure exerted by soil when it is laterally compressed to the point of failure, which was calculated using the expression $K_p = (1 + \sin\phi'_{cr})/(1 - \sin\phi'_{cr})$. As suction decreases from 804 kPa to 200 kPa, the stress path shifts away from K_o to K_p whilst illustrating a significantly greater variation in vertical Bishop's stress σ^*_z in comparison to the horizontal Bishop's stress σ^*_x. This is due to the fact that, in the horizontal direction the effects of reduced suction stress ($S_{eff}s$) on σ^*_x were compensated for by an almost equal increase in horizontal total stress since the presence of the pile prevents lateral straining. Conversely, in the vertical direction, soil elements are allowed to swell more freely. As a result, vertical total stress remains largely unchanged while the effects of $S_{eff}s$ dissipate, producing the observed reduction in σ^*_z. This mechanism is further supported by the fact that, at greater depths where overburden pressure suppresses swell to a certain extent, the observed reductions in σ^*_x were even lower (see for soil element U3). However, once the stress paths approach the K_p line, passive failure of adjacent soil elements produces the observed reductions in σ^*_x with further reductions in $S_{eff}s$.

Case 2: Free-standing Pile under Hydraulic Loading

Fig. 9 illustrates how the propagation of a wetting front under different hydraulic boundary conditions influences the evolution of swell. The wetting front is depicted as the change in $S_{eff}s$ at various degrees of swell (Lu 2008; Lu and Likos 2006). During RWT scenario, water infiltrates from the soil base leading the wetting front to propagate upward. This causes suction loss and an increase in degree of saturation showing an overall reduction in $S_{eff}s$ (Fig. 9(a)). In contrast, for RI condition, starting from the ground surface as water infiltrates, the wetting front

moves downward causing successive reduction in $S_{eff}s$ (Fig. 9(b)). The advancement of the wetting front and the associated swell development significantly influence the mobilization of shaft friction along the pile. As an example, a detailed overview of the swell distribution at the targeted swell $\Delta h/\Delta h_f$ = 0.42 for the RWT and RI conditions is highlighted in Appendix S4.

Fig. 10 illustrates how hydraulic boundary conditions influence the mechanical behavior of a single pile. In Fig. 10(a), shaft friction along the pile length is presented for two swell levels: $\Delta h/\Delta h_f$ = 0.18 and 1. The advancement of the wetting front under RI conditions causes suction loss and resulting swell at shallow depth, leading to a lower mobilization of shaft resistance when compared to RWT condition ($\Delta h/\Delta h_f$ = 0.18). However, below the neutral axis, higher shaft friction remains until wetting front reaches the pile base ($\Delta h/\Delta h_f$ = 1). This distribution of shaft friction affects the pile axial load as shown in Fig. 10(b), where RWT conditions generate a higher pile axial load above the neutral axis than the RI scenario. This indicates that an RWT leads to more pronounced pull-out effects.

Case 3: Combined Mechanical and Hydraulic Loading

The estimates of ultimate load capacity Q_{ult} of pile foundation based on saturated soil mechanics are often conservative, as they do not consider suction effects in unsaturated soils (Lalicata et al. 2019; Lalicata et al. 2022). Field pile load tests conducted under such conditions provide a more accurate assessment of pile capacity. Q_{ult} can be determined through various methods applied to the load-displacement response data from in-situ pile load tests. One widely used method is the double tangent approach (Butler and Hoy 1977) which was used in this study, to determine Q_{ult} for both saturated and unsaturated conditions. To estimate Q_{ult} for unsaturated conditions (unswelled state), a pile load test was simulated using 3D-FE model, where a single pile was subjected to vertical downward displacement at the pile head to generate the load-displacement response as shown in Fig. 11.

At an unswelled state, Q_{ult} was estimated equal to 1350 kN, yielding an allowable load capacity $Q_{a\text{-}unsat}$ = 450 kN using a factor of safety, FOS = 3 (BIS 2010). At the final swell level of 6% (close to saturated condition, s = 0 kPa), Q_{ult} decreased to 250 kN, resulting in $Q_{a\text{-}sat}$ of 83 kN. For comparison, $Q_{a\text{-}sat}$ was also calculated using the β method (Chandler 1968; Burland 1973) including the contribution of end bearing (BIS 1981). This analysis yielded an estimated $Q_{a\text{-}sat}$ = 80 kN with a FOS of 3, which closely aligned with the capacity obtained from the 3D-FE model for a final swell of 6%.

Further comparison of design capacities under both unsaturated and saturated conditions shows that unsaturated clays provide approximately 5.4 times greater pile capacity. This is similar to the field observation reported by Elsharief et al. (2007) where authors reported a pile capacity 3 times higher for a pile embedded in expansive clays under unswelled conditions compared to the capacity achieved after swelling was induced. It should be noted that in-situ soil state is constantly influenced by changing flux boundary conditions, which can significantly influence the results of field pile load testing. For instance, two pile load tests simulated using a 3D-FE model at targeted swell of 2.5% achieved under RWT and RI conditions displayed different load-settlement response (Fig. 11). Table 4 summarizes a comparison of pile capacities, for different levels of swell, where the soil profile was subjected to different hydraulic conditions. Further investigation was conducted to analyse the performance of a single pile under allowable loads of $Q_{a\text{-}sat}$ = 80 kN and $Q_{a\text{-}unsat}$ = 450 kN, subjected to RWT and RI conditions. Fig. 12(a) illustrates the variation in axial load with depth during swelling for a single pile carrying 80 kN. The development of tensile load within the pile was observed during swelling, with higher magnitudes under RWT compared to RI. The greatest difference occurred above the neutral plane at a low degree of swell ($\Delta h/\Delta h_f$ = 0.18), which diminished as swelling progressed ($\Delta h/\Delta h_f$ = 1), although the pile continued to experience tensile stresses at the end of swell. The external compressive load counteracted the swell-induced loading, shifting the neutral plane downward

and reducing the tensile axial load within the pile as compared to the free-standing pile case (Fig. 10(b)). This effect became more pronounced under the higher load of 450 kN (Fig. 12(b)). Notably, under the lighter compressive load, predominantly tensile stresses were present within the pile, even at $\Delta h/\Delta h_f = 1$ (Fig. 12(a)), However, under 450 kN, a greater portion of the pile was under compression at $\Delta h/\Delta h_f = 0.18$ (more pronounced in the RI case), and at $\Delta h/\Delta h_f = 1$ the pile was entirely under compression.

Fig. 12(c) shows that the pile experiences uplift under 80 kN, regardless of the wetting condition. However, under the RI condition uplift is reduced, primarily due to the anchoring effect of negative shaft friction and higher suction at depth. This anchoring effect remains significant until the wetting front reaches the pile base, leading to a reduction in suction. Fig. 12(d) illustrates that uplift was unavoidable even under the higher load of 450 kN, primarily due to the significant swelling pressures generated in expansive clays at low swelling degrees (Gaspar et al. 2022) and the development of positive shaft friction. However, as swelling progresses, the pile transitions from uplift to settlement at higher swell magnitudes ($\Delta h/\Delta h_f =$ 0.5 for RWT and $\Delta h/\Delta h_f = 0.75$ for RI). This shift occurs at higher swell magnitudes due to swell-induced softening and significant loss of suction ($s = 75$ kPa at $\Delta h/\Delta h_f = 0.5$ for RWT and $s = 28$ kPa $\Delta h/\Delta h_f = 0.75$ for RI) which acted together to reduce pile shaft capacity. The point at which this transition in pile movement occurs can be interpreted as the instance at which the net pullout effect of the positive shaft resistance is reduced to a value less than the applied load of 450 kN.

These findings suggest that the tendency of conventional methods to underestimate pile shaft capacity can lead to erroneous predictions in the direction (uplift or settlement) and magnitude of pile movement during a swell process. Furthermore, conventional methods do not allow for the assessment of the stress state of the pile (whether in compression or tension), or the

magnitude of induced pile loading during a swell process. Therefore, consideration of the unsaturated case should be employed to provide a more rational estimation of pile behavior.

Discussion on Field Application and Limitations of the Study

Overall, this study highlights the effects of suction loss coupled with swelling and swell-induced softening on the response of a single pile embedded in the active zone of a highly expansive clay. The findings demonstrate that the suction within the clay profile plays a significant role in the mobilization of shaft resistance and pile displacements, in a way that is often overlooked in conventional design approaches. Once suction is reduced below the air occlusion (AOV) value, the effects of swell-induced softening become apparent, with a dramatic reduction in shaft capacity (a loss in shaft friction of about 85% from AOV to full saturation) (Fig. 7(b)). Furthermore, the magnitude of swell during suction dissipation governs the development of tensile loading in the pile as a neutral plane develops around its mid-length ($0.5L$ –$0.55L$).

Importantly, only a relatively small amount of swell (degree of swell of 18%) is sufficient to induce the maximum tensile loading in the pile. This ‘pre-loading’ effect pre-stresses the pile in tension, reducing reserve capacity available to sustain design tensile loads. This can be detrimental for lightly loaded piles, piles subjected to lateral loading or tension piles. Also, the pile uplift brought by swelling is dictated by the magnitude of compressive loading, a phenomenon can only be accounted by considering unsaturated soil mechanics principles.

In the absence of sophisticated finite element modeling or in-situ testing, the study has shown that limiting values of swell-induced shaft friction can reasonably be estimated using CPT data and the approach outlined by Eslami and Fellenius (1997). Furthermore, changes in suction and swell-induced softening were found to be most critical for a rising water table condition, as such a scenario affects greater portions of the clay profile. Conversely, it was shown that

pile behavior was less affected by rainfall infiltration due to a much shallower depth of influence.

Although, the chosen constitutive model captured key aspects of the pile behavior under unsaturated and swelled conditions, it is important to highlight that the effect of fissuring was only accounted for implicitly. Field testing together with a detailed monitoring scheme has the potential to better explain the coupled impact of suction and swelling on the response of piled foundations. However, such programs are costly, and inevitably suffer from difficulties related to measurements of soil suction. Nonetheless, this study could capture key aspects of pile behavior in swelling soil with reasonable accuracy. This work can be extended to understand pile response under cycles of hydraulic loading and for different loading configurations such as laterally loaded piles.

Conclusions

This study investigated the response of a single pile embedded in a high-plasticity South African expansive clay under both unswelled conditions, and varying degrees of swelling. Specifically, numerical modeling was performed using the Barcelona Basic Model to quantify the contribution of suction in controlling the response of a single pile prior to swell, and throughout the swell process. To validate the numerical model, the results of centrifuge testing were used in benchmarking studies. The centrifuge modeling considered in this study, investigated both the evolution of swell in a deep clay profile under greenfield conditions, and the effects of swell on pile shaft capacity. The numerical model successfully replicated the free-swell behavior observed in the greenfield centrifuge test, accurately capturing the magnitude, rate, and spatial and temporal variations in swell evolution. The model also reproduced the response of a single pile subjected to pull-out tests under both unswelled and targeted surface swell conditions. Results show that swell-induced softening caused a reduction of approximately 50% in peak shaft capacity under targeted swell levels compared to unswelled

596 conditions. Following validation against centrifuge testing, a parametric study was conducted
597 to further investigate the behavior of single pile foundation under various hydraulic loading
598 scenarios, both with and without applied mechanical loading at the pile head.
599 Key findings for each analysis are summarized below:
600 (a) Case 1: Free-standing pile: Contrary to previous studies, the results demonstrated the
601 formation of a neutral plane (NP) within the active zone, where positive and negative shaft
602 friction were mobilized above and below the NP, respectively. This led to the development of
603 a maximum tensile axial load at the NP, the magnitude of which was dictated by variations in
604 suction, lateral swell pressure and swell-induced softening. The limiting tensile load occurred
605 at approximately 18% of the total swell and was closely related to the evolution of the stress
606 path during wetting. Swell-induced softening was found to be the dominant mechanism at
607 suctions below the air-occlusion value, ultimately causing the observed reduction in axial pile
608 load.
609 (b) Case 2: Free-standing pile under hydraulic loading: The propagation of the wetting front
610 dictated the swell evolution which significantly impacted the mechanical behavior of the pile.
611 Results showed that the suction loss and resulting swell was concentrated near the ground
612 surface during rainfall infiltration (RI), whereas during the rise in water table (RWT) scenario,
613 the swell contours were more evenly distributed throughout the soil profile. This indicates that
614 a RWT leads to more pronounced pull-out effects and as a result, generated higher tensile axial
615 loads within the pile in comparison to RI scenario.
616 (c) Case 3: Combined mechanical and hydraulic loading: The external compressive load
617 counteracted the swell-induced ‘pull-out’ loading, shifting the NP downward and reducing the
618 axial tensile load within the pile in comparison to the free-standing pile case under hydraulic
619 loading (Case 2). Moreover, this effect became more pronounced under the higher applied load
620 (equivalent to allowable load in unsaturated conditions). However, pile uplift remined

unavoidable due to the build-up of significant lateral swelling pressure and positive shaft friction during initial swell from a high value of suction. As swelling progressed, the pile was seen to transition from uplift to settlement at higher swell magnitudes due to the increasing effects of swell-induced softening.

The study also highlighted the conservatism in calculating pile capacity based on saturated soil mechanics, with the capacity found to be approximately five times lower than unsaturated pile capacity as evidenced by the simulated field tests. The outcome of this study enhances the understanding of the coupled effect of swelling and suction in dictating the overall response of pile foundations.

Supplemental Materials

Appendix S1-S4 are available online in the ASCE Library (www.ascelibrary.org).

Data Availability Statements

All the relevant data and models used in this study have been provided in the form of Figures and Tables. Additional data generated from analysis and models are available from the corresponding author upon reasonable request.

Acknowledgements

This work was funded by the UK Engineering and Physical Sciences Research Council (EPSRC) under the Global Challenges Fund programme for a project entitled ‘Developing Performance based design for foundations of wind turbines in Africa (WindAfrica)’, Grant Ref: EP/P029434/1. The first author acknowledges the financial support received from the Commonwealth Scholarship Commission in the UK, Government of the United Kingdom. The scholarship was granted under the Ph.D. Commonwealth Split-site Scholarship reference number INCN-2023-196.

References

Abdollahi, M., and F. Vahedifard. 2021. “Model for lateral swelling pressure in unsaturated expanive soils.” *J. Geotech. Geoenviron. Eng.* 147 (10): 04021096. https://doi.org/10.1061/(ASCE)GT.1943-5606.0002605.

Al-Dakheeli, H., and R. Bulut. 2019. “Interrelationship between elastic deformation and soil-water characteristic curve of expansive soils.” *J. Geotech. Geoenviron. Eng.* 145 (4): 04019005. https://doi.org/10.1061/(ASCE)GT.1943-5606.0002020.

Alonso, E. E., A. Gens, and A. Josa. 1990. “A constitutive model for partially saturated soils.” *Géotechnique* 40 (3): 405–430.

ASTM (American Society for Testing and Materials). 2010. *Standard Test Method for Measurement of Soil Potential (Suction) Using Filter Paper*. ASTM D5298-10. West Conshohocken, PA: ASTM.

Azizi, A., A. Kumar, M. I. Lingwanda, and D. G. Toll. 2020. “The influence of rates of drying and wetting on measurements of soil water retention curves.” *E3S Web of Conferences*, 195: 03005. https://doi.org/10.1051/e3sconf/202019503005.

Benvenga, M. M. 2005. “Pier-soil adhesion factor for drilled shaft piers in expansive soil.” Master’s thesis, Colorado State Univ., Fort Collins, CO.

Bilotta, E., and S. E. Stallebrass. 2009. “Prediction of stresses and strains around model tunnels with adjacent embedded walls in overconsolidated clay.” *Comput. Geotech.*, 36(6): 1049-1057. https://doi.org/10.1016/j.compgeo.2009.03.015

BIS (Bureau of Indian Standards). 1981. *Indian Standard Determination of Bearing Capacity of Shallow Foundations - Code of Practice (First Revision)*. IS 6403. New Delhi: BIS.

BIS (Bureau of Indian Standards). 2010. *Indian Standard Design and Construction of Pile Foundations - Code of Practice Part 1 Concrete Piles Section 2 Bored Cast In-situ Concrete Piles (Second Revision)*. IS 2911-1-2. New Delhi: BIS.

Blight, G. E. 1984. “Power station foundations in deep expansive soil.” In *Proceedings of the First International Conference on Case Histories in Geotechnical Engineering, Missouri*. 77–86.

BSI (British Standards Institution). 2009. *Testing hardened concrete – Tensile splitting strength of test specimens.* BS EN 12390-6. British Standards Institution, London, UK.

BSI (British Standards Institution). 2013. *Testing hardened concrete – Determination of secant modulus of elasticity in compression.* BS EN 12390-13. British Standards Institution, London, UK.

BSI (British Standards Institution). 2019. *Testing hardened concrete – Compressive strength of test specimens.* BS EN 12390-3. British Standards Institution, London, UK.

Burland, J. 1973. “Shaft friction of piles in clay–a simple fundamental approach.” *Ground Eng.* 6 (3): 30–42.

Butler, H. D., and H. E. Hoy. 1977. “User manual for taxes quick-load method for foundation load testing.” FHWA-IP-77-8. Washington, DC: Federal Highway Administration.

Byrne, G., N. Chang, and V. Raju. 2019. A guide to practical geotechnical engineering in Africa (5th ed.). FRANKI A KELLER COMPANY, Olifantsfontein.

Caicedo, B., C. Medina, and A. Cacique. 2006. “Validation of time scale factor of expansive soils in centrifuge modeling.” In *Int. Conf. Phys. Modelling in Geotechnics* 06: 273–277.

Challa, P. K., and H. G. Poulos. 1991. “Behaviour of single pile in expansive clay.” *Geotech. Eng.* 22 (2): 189–216.

Chandler, R. J. 1968. “The shaft friction of piles in cohesive soils in terms of effective stress.” *Civ. Eng. Public Works Rev.* 60: 48–51.

Chen, F. H. 1975. Foundations on expansive soils. Amsterdam, Netherlands: Elsevier.

694 Conti, R., G. M. Viggiani, and F. Perugini. 2014. “Numerical modelling of centrifuge dynamic
695 tests of circular tunnels in dry sand.” *Acta Geotech.*, 9: 597-612.
696 https://doi.org/10.1007/s11440-013-0286-8
697 da Silva Burke, T. S., S. W. Jacobsz, M. Z. E. B. Elshafie, and A. S. Osman. 2022.
698 “Measurements of pile uplift forces due to soil heave in expansive clay.” *Can. Geotech.*
699 *J.* 59 (12): 2119–2134. https://doi.org/10.1139/cgj-2021-0079.
700 Elsharief, A. M., E. O. Ahmed, and Y. E. A. Mohamedzein. 2007. “Guidelines for the design
701 of bored concrete piles in expansive soils of Sudan.” In *Grad. Sch. Conf. Basic Sci. Eng.*,
702 Univ. of Khartoum, Khartoum.
703 Elsharief, A. 2012. “Foundations on expansive soils, Sudan experience.” *Grad. Sch. Conf.*
704 *Basic Sci. Eng.*, Univ. of Khartoum, Khartoum.
705 Esmaili, D., and K. Hatami. 2017. “Comparative study of measured suction in fine-grained soil
706 using different in-situ and laboratory techniques.” *Int. J. Geosynth. Ground Eng.* 3, 27.
707 Fan, Z. -h., Y. -h. Wang, H. -b. Xiao, and C. -s. Zhang. 2007. “Analytical method of load-
708 transfer of single pile under expansive soil swelling.” *J. Cent. South Univ. Technol.* 14:
709 575–579. https://doi.org/10.1007/s11771-007-0110-4.
710 Fredlund, D. G., D. Sheng, and J. Zhao. 2011. “Estimation of soil suction from soil-water
711 characteristic curve.” *Can. Geotech. J.* 48: 186–198.
712 Galavi, V. 2010. *Groundwater flow fully coupled flow deformation and undrained analyses in*
713 *PLAXIS 2D and 3D*. Internal report, Research Department, Plaxis BV.
714 Gaspar, T. A. V. 2020. *Centrifuge modelling of piled foundations in swelling clays* (PhD
715 thesis). University of Pretoria, Pretoria, South Africa.
716 Gaspar, T. A. V., S. W. Jacobsz, G. Heymann, D. G. Toll, A. Gens, and A. S. Osman. 2022.
717 “The mechanical properties of a high plasticity expansive clay.” *Eng. Geol.* 303: 106647.
718 https://doi.org/10.1016/j.enggeo.2022.106647.

719 Gaspar, T. A. V., S. W. Jacobsz, G. Smit, A. Gens, D. G. Toll, and A. S. Osman. 2023.
720 “Centrifuge modelling of an expansive clay profile using artificial fissuring to accelerate
721 swell.” *Eng. Geol.* 312: 106928. https://doi.org/10.1016/j.enggeo.2022.106928.
722 Gaspar, T. A. V., S. W. Jacobsz, G. Smit., and A. S. Osman. 2024. “Centrifuge modelling of
723 piled foundations in swelling clays.” *Can. Geotech. J.* 61 (1): 1–13.
724 https://doi.org/10.1139/cgj-2022-0449.
725 Gens, A., and E. E. Alonso. 1992. “A framework for the behaviour of unsaturated expansive
726 clays.” *Can. Geotech. J.* 29 (6): 1013–1032.
727 Gens, A. 2010. “Soil-environment interactions in geotechnical engineering.” *Géotechnique* 60
728 (1): 3–74.
729 Jacobsz, S. W., E. P. Kearsley, and J. H. L. Kock. 2014. “The geotechnical centrifuge facility
730 at the University of Pretoria.” In *Physical Modelling in Geotechnics: Proceedings 8th*
731 *ICPMG, C. Gaudin & D. White (eds)*. 169–174, CRC Press.
732 Jaky, J. 1944. “The coefficient of earth pressure at rest.” *J. Soc. Hungarian Archit. Eng.* 355–
733 358.
734 Jennings, J. E., and J. E. Kerrich. 1962. “The heaving of buildings and the associated economic
735 consequences with particular reference to the Orange Free State Goldfields.” *Civ. Eng. S.*
736 *Afr.* 4 (11): 221–248.
737 Jiang, J., K. Hou, and X. Ou. 2020. “Analysis of the bearing capacity of a single pile based on
738 an analytical solution of pile–soil interaction in expansive soil.” *Geotech. Geol. Eng.* 38:
739 1721–1732. doi:10.1007/s10706-019-01126-2.
740 Kumar, S., and A. Kumar. 2023. “Effect of infiltration on single-pile and monopile-raft
741 foundation embedded in unsaturated sand.” *Int. J. Geomech.* 23(2): 04022288.
742 https://doi.org/10.1061/ijgnai.gmeng-7908.

743 Lalicata, L.M., A. Desideri, F. Casini, and L. Thorel. 2019. “Experimental observation on
744 laterally loaded pile in unsaturated silty soil.” Can. Geotech. J. 56: 1545–1556.
745 Lalicata, L. M., G. M. Rotisciani, A. Desideri, and F. Casini. 2022. “A numerical model to
746 study the response of piles under lateral loading in unsaturated soils.” *Geosciences.* 12(1),
747 1. https://doi.org/10.3390/geosciences12010001
748 Lalicata, L. M., E. Ritchie, S. E. Stallebrass, and A. McNamara. 2024. “Novel experimental
749 technique to model impression piles in centrifuge testing.” *Int. J. Phys. Model. Geotech.*
750 24(2): 78-91. https://doi.org/10.1680/jphmg.22.00065
751 Lalicata L. M., S. E. Stallebrass, and A. McNamara. 2023. “An experimental study into the
752 ultimate capacity of an ‘impression’ pile in clay. Géotechnique 73(5): 455–466.
753 https://doi.org/10.1680/jgeot.21.00168
754 Li, J., D. Cameron, and G. Ren. 2014. “Case study and back analysis of a residential building
755 damaged by expansive soils.” *Comput. Geotech.* 56: 89–99.
756 Liu, Y., and S. K. Vanapalli. 2019. “Load displacement analysis of a single pile in an
757 unsaturated expansive soil.” *Comput. Geotech.* 106: 83–98.
758 Liu, Y., and S. K. Vanapalli. 2022. “Modified shear displacement method for analysis of piles
759 in unsaturated expansive soils considering influence of environmental factors.” *Int. J.*
760 *Geomech.* 22 (6): 04022069.
761 Lloret, A., M. V. Villar, M. Sanchez, A. Gens, X. Pintado, and E. E. Alonso. 2003. **“**Mechanical
762 behaviour of heavily compacted bentonite under high suction changes.” *Géotechnique*,
763 53(1): 27–40.
764 Louw, H., E. Kearsley, and S. W. Jacobsz. 2022. “Modelling horizontally loaded reinforced-
765 concrete piles in a geotechnical centrifuge.” *Int. J. Phys. Model. Geotech.* 22(1): 14–25,
766 https://doi.org/10.1680/jphmg.20.00016

767 Lu, N. 2008. “Is matric suction a stress variable?” *J. Geotech. Geoenviron. Eng.* 134 (7): 899–
768 905. https://doi.org/10.1061/(ASCE)1090-0241(2008)134:7(899).
769 Lu, N., and W. J. Likos. 2006. “Suction stress characteristic curve for unsaturated soil.” *J.*
770 *Geotech. Geoenviron. Eng.* 132 (2): 131–142. https://doi.org/10.1061/(ASCE)1090-
771 0241(2006)132:2(131).
772 Meter Group. 2017a. *5TM User’s Manual*. Meter Group.
773 Meter Group. 2017b. *Teros 21. User Manual*. Meter Group.
774 Nelson, J. D., E. G. Thompson, R. W. Schaut, K-C., Chao, D. D. Overton, and J. S. Dunham-
775 Friel. 2012. “Design procedure and considerations for piers in expansive soils.” *J.*
776 *Geotech. Geoenviron. Eng.* 138 (8): 945–956.
777 Panchal, J. P., and A. M. McNamara. 2018. “Federation of piling specialists’ casing extraction
778 review.” *Proc. ICE Geotech. Eng*. 171(2): 174-185.
779 Pham T. A., S. Nadimi, and M. Sutman. 2024. “Softening-based interface model and nonlinear
780 load-settlement response analysis of piles in saturated and unsaturated multi-layered
781 soils.” *Comput. Geotech.* 171: 106331.
782 PLAXIS. 2023a. *User Defined Soil Model - BBM: Barcelona Basic Model in PLAXIS*,
783 Computer software, Delft, Netherlands.
784 PLAXIS. 2023b. *Material Models Manual*, Computer software, Delft, Netherlands.
785 PLAXIS. 2023c. *Reference Manual*, Computer software, Delft, Netherlands.
786 Poulos, H. G. 1989. *Program PIES Axial Response of Piles in Expansive Soils*. Centre for
787 Geotechnical Research, University of Sydney, Sydney, NSW.
788 Rotisciani, G. M., F. Casini, A. Desideri, and G. Sciarra. 2017. “Hydromechanical behavior of
789 an embankment during inundation.” *Can. Geotech. J.*, 54(3), 348-358.
790 https://doi.org/10.1139/cgj-2016-0174

Smit, G., T. A. V. Gaspar, S. W. Jacobsz, and A. S. Osman. 2019. “Centrifuge modelling of pile pull-out tests in expansive soil.” In *XVII European Conference on Soil Mechanics and Geotechnical Engineering*, Reykjavik, Iceland.

Song, Z. 2008. *Pullout behaviour of suction embedded plate anchors in clay* (Ph.D. thesis). Curtin University, Perth, Australia.

Soranzo, E., R. Tamagnini, and W. Wu. 2015. “Face stability of shallow tunnels in partially saturated soil: Centrifuge testing and numerical analysis.” *Géotechnique*, 65: 454–467.

Tavenas, F., P. Jean, P. Leblond, and S. Leroueil. 1983. “The permeability of natural soft clays. Part II: permeability characteristics.” *Can. Geotech. J.* 20: 645–660. https://doi.org/10.1139/t83-073.

Terzaghi, K. 1925. Principles of soil mechanics: I- Phenomena of cohesion of clays. *Eng. News-Record* 95 (19): 742–746.

Tripathy, S., K. S. Subba Rao, and D. G. Fredlund. 2002. “Water content–void ratio swell–shrink paths of compacted expansive soils.” *Can. Geotech. J.*, 39: 938–959.

Van der Merwe, D. 1964. “The prediction of heave from the plasticity index and percentage clay fraction of soils.” *The Civil Engineer*, 103–107.

van Genuchten, M. T. 1980. “A closed-form equation for predicting the hydraulic conductivity of unsaturated soils.” *Soil Sci. Soc. Am. J.* 44 (5): 892–898.

Wu, X., and S. K. Vanapalli. 2022. “Three-dimensional modeling of the mechanical behavior of a single pile in unsaturated expansive soils during infiltration.” *Comput. Geotech.* 145: 104696.

Xiao, H. -b., C. -s. Zhang, Y. -h. Wang, and Z. -h. Fan. 2011. “Pile–soil interaction in expansive soil foundation: analytical solution and numerical simulation.” *Int. J. Geomech.* 11: 159–166. doi:10.1061/(ASCE)GM.1943-5622.0000046.

Figure Caption

Fig. 1. Pile-soil-swell mechanism of single pile in expansive clay during swelling.

Fig. 2. Schematic diagram of centrifuge model used for (a) free swell mechanism (b) pile pull-out response.

Fig. 3. Details of 3D-FE models used for (a) free swell mechanism (b) pile pull-out response.

Fig. 4. VG model parameters (a) SWRC (b) k_{sat} and c_k in k_{sat} : e space

Fig. 5. Comparison of 3D-FE modeling and centrifuge testing (a) surface swell with time (b) swell with normalized depth below ground.

Fig. 6. Comparison of 3D-FE modeling and centrifuge testing (a) surface swell with time (b) shaft friction with normalized displacement.

Fig. 7. Variation along the pile length for (a) normalized pile-soil relative displacement (b) shaft friction (c) axial load

Fig. 8. During swelling the variation of (a) maximum pile tensile axial load (b) stress path for elements at pile-soil interface

Fig. 9. Propagation of wetting front during (a) RWT (b) RI

Fig. 10. Effect of hydraulic boundary conditions on (a) shaft friction (b) pile axial load

Fig. 11. Load-settlement response of single pile

Fig. 12. Effect of hydraulic boundary on (a) axial load under 80 kN (b) axial load under 450 kN (c) pile uplift under 80 kN (d) pile uplift under 450 kN

841 **List of Tables**

842 **Table 1.** Material properties of model pile

843 **Table 2.** Analysis sequence during centrifuge testing and 3D-FE modeling

844 **Table 3.** Barcelona Basic Model (BBM) and interface model parameters used in numerical

845 modeling

846 **Table 4.** Capacity of pile foundation under different levels of swell

1 Table 1. Material properties of model pile

	Grout	Testing standard/reference
Compressive strength (MPa)	35.87	BSI (2019)
Indirect tensile strength (MPa)	2.30	BSI (2009)
Young's modulus (GPa)	11.90	BSI (2013)
Density (kg/m^3)	1920	-

2

Click here to access/download;Table;Table 2.docx

Table 2. Analysis sequence during centrifuge testing and 3D-FE modeling

Phase	Free swell prediction – Centrifuge	Free swell prediction – 3D-FE	Pile pull-out response – Centrifuge	Pile pull-out response – 3D-FE
Initial	Gravity increased from 1g to 30g	Initialization of effective stresses at prototype scale	Installation of model piles at 1g	Initialization of effective stresses at prototype scale
Phase 1	Water introduced from bottom, rising through side wells and geotextile; added for 30 min until water reached 20 mm depth at surface	Zero-pore pressure activated sequentially (bottom to top) with a standing water head of 0.6 m over 900 minutes	Gravity increased from 1g to 30g	Activation of piles and interface elements
Phase 2	Continued flooding with access to water from top,	Zero-pore pressure maintained to allow swell	Pull-out test conducted on Piles 2 & 4 in	Pull-out simulation for Piles 2 & 4 in

	bottom, and side wells maintained for 110 hours	development via coupled consolidation for 4125 days	unswelled condition	unswelled condition
Phase 3	–	–	Water introduced as in Phase 1 for free swell test; continued for 30 minutes until water level reached 20 mm above surface of model.	Zero-pore pressure activated as in Phase 1 for free swell test for 900 minutes
Phase 4	–	–	Flooding conditions sustained for 10 hours until targeted surface swell of 5 mm was achieved	Zero-pore pressure maintained to simulate swell via coupled consolidation for 375 days

Phase 5	–	–	Pull-out test executed on Piles 1 & 3 at the targeted surface swell condition	Pull-out simulation for Piles 1 & 3 under targeted swell condition

2

Click here to access/download;Table;Table 3.docx

Table 3. Barcelona Basic Model (BBM) and interface model parameters used in numerical modeling

Mechanical model		Hydromechanical model		Interface model	
Parameter	Value	Parameter	Value	Parameter	Value
Poisson's ratio, ν' (-)	0.25	Initial degree of saturation, S_{inl} (-)	0.965	Reference stiffness for primary oedometer loading, E_{oed}^{ref} (kN/m^2)	1865
Slope of normal compression line (υ : ln p' space), λ (-)	0.13	Residual degree of saturation, S_{res} (-)	0.30	Reference pressure, p^{ref} (kN/m^2)	100
Slope of swelling line (υ : ln p' space), κ (-)	0.035	Fitting parameter controlling the air entry value, g_a (m^{-1})	0.005	Rate of stress dependency of the interface stiffness m (-)	0.5
Critical state friction angle, ϕ'_{cr} (°)	17.78	Fitting parameter controlling the rate of water	2.5	Effective interface friction angle, δ'_{int} (°)	17.78

		extraction/imbibition, g_n (-)			
Coefficient of plastic potential for non-associated flow rule, α (-)	0.37	Fitting parameter equal to (1- g_n) / g_n, g_c (-)	-0.6	Effective interface cohesion, c'_{int} (kN/m^2)	0
Reference effective pressure, p'_r (kPa)	1.0	Permeability change index, c_k (-)	0.5		
Slope of swelling line (υ : ln s space), κ_s (-)	0.027	Coefficient of saturated hydraulic conductivity, k_{sat} (m/day)	8.64×10^{-8}		
Parameter for increase in apparent cohesion with suction, k_s (-)	0.29				
Parameter controlling changes in soil	0.8				

stiffness with suction, r (-)					
Parameter controlling rate of increase in soil stiffness with suction, β (kPa^{-1})	0.012				

3

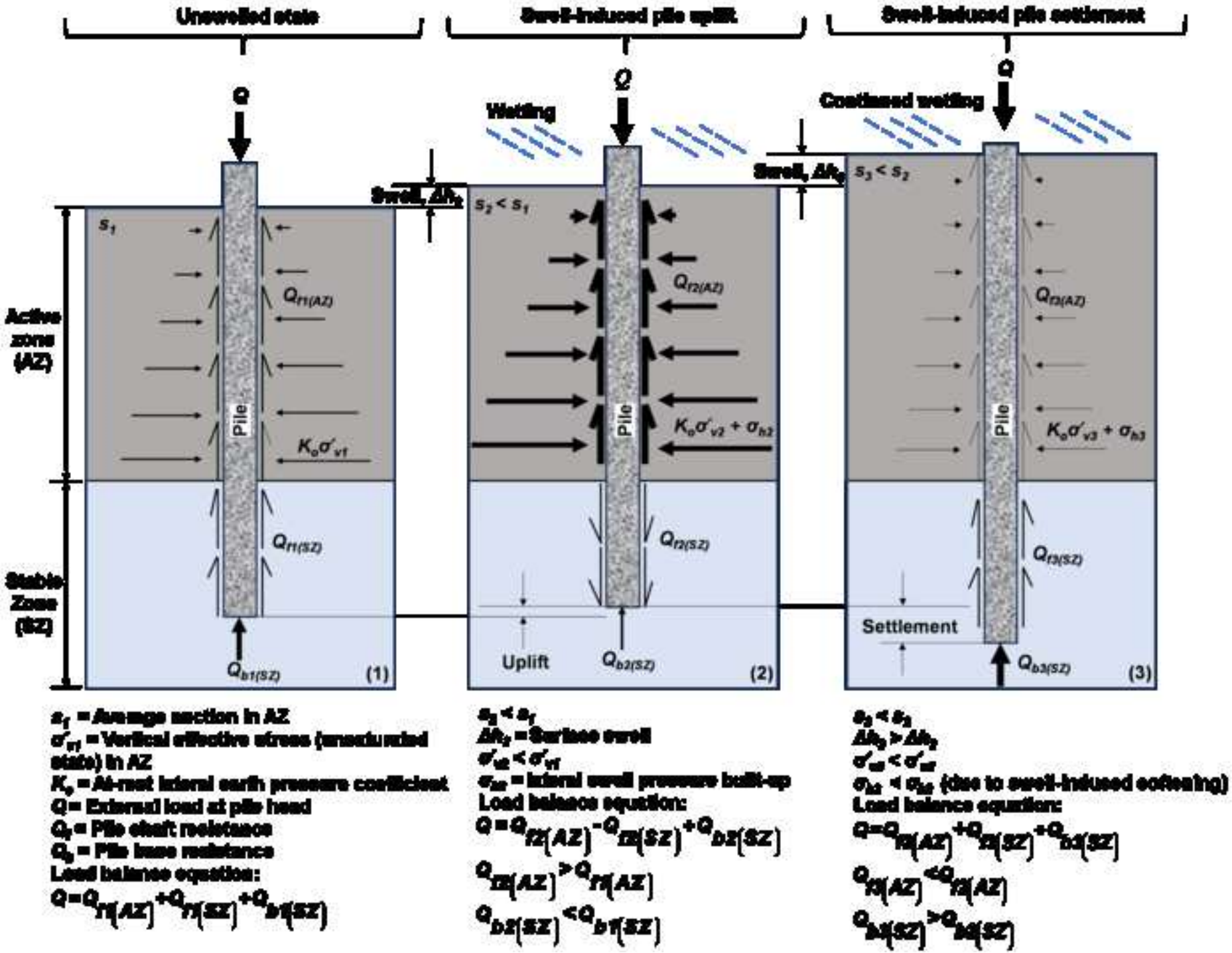
Click here to access/download;Table;Table 4.docx

Table 4. Capacity of pile foundation under different levels of swell

Hydraulic path	Unswelled state	Rainfall Infiltration (RI)		Rise in Water Table (RWT)	
Degree of swell ($\Delta h/\Delta h_f$)	0%	2.5%	6.0%	2.5%	6.0%
Ultimate load Q_{ult} (kN)	1350	865	250	750	250
Allowable load Q_a (kN)	450	288	83	250	83

Fig. 1

Click here to access/download;Figure;Fig. 1.tif



s_1 = Average section in AZ
σ'_{v1} = Vertical effective stress (unsaturated state) in AZ
K_o = At-rest lateral earth pressure coefficient
Q = External load at pile head
Q_f = Pile shaft resistance
Q_b = Pile base resistance
Load balance equation:

$$Q = Q_{f1(AZ)} + Q_{f1(SZ)} + Q_{b1(SZ)}$$

$s_2 < s_1$
Δh_2 = Surface swell
$\sigma'_{v2} < \sigma'_{v1}$
σ_{h2} = lateral swell pressure built-up
Load balance equation:

$$Q = Q_{f2(AZ)} - Q_{f2(SZ)} + Q_{b2(SZ)}$$

$$Q_{f2(AZ)} > Q_{f1(AZ)}$$

$$Q_{b2(SZ)} < Q_{b1(SZ)}$$

$s_3 < s_2$
$\Delta h_3 > \Delta h_2$
$\sigma'_{v3} < \sigma'_{v2}$
$\sigma_{h3} < \sigma_{h2}$ (due to swell-induced softening)
Load balance equation:

$$Q = Q_{f3(AZ)} + Q_{f3(SZ)} + Q_{b3(SZ)}$$

$$Q_{f3(AZ)} < Q_{f2(AZ)}$$

$$Q_{b3(SZ)} > Q_{b2(SZ)}$$

Fig. 2(a)

Click here to access/download;Figure;Fig. 2(a).tif

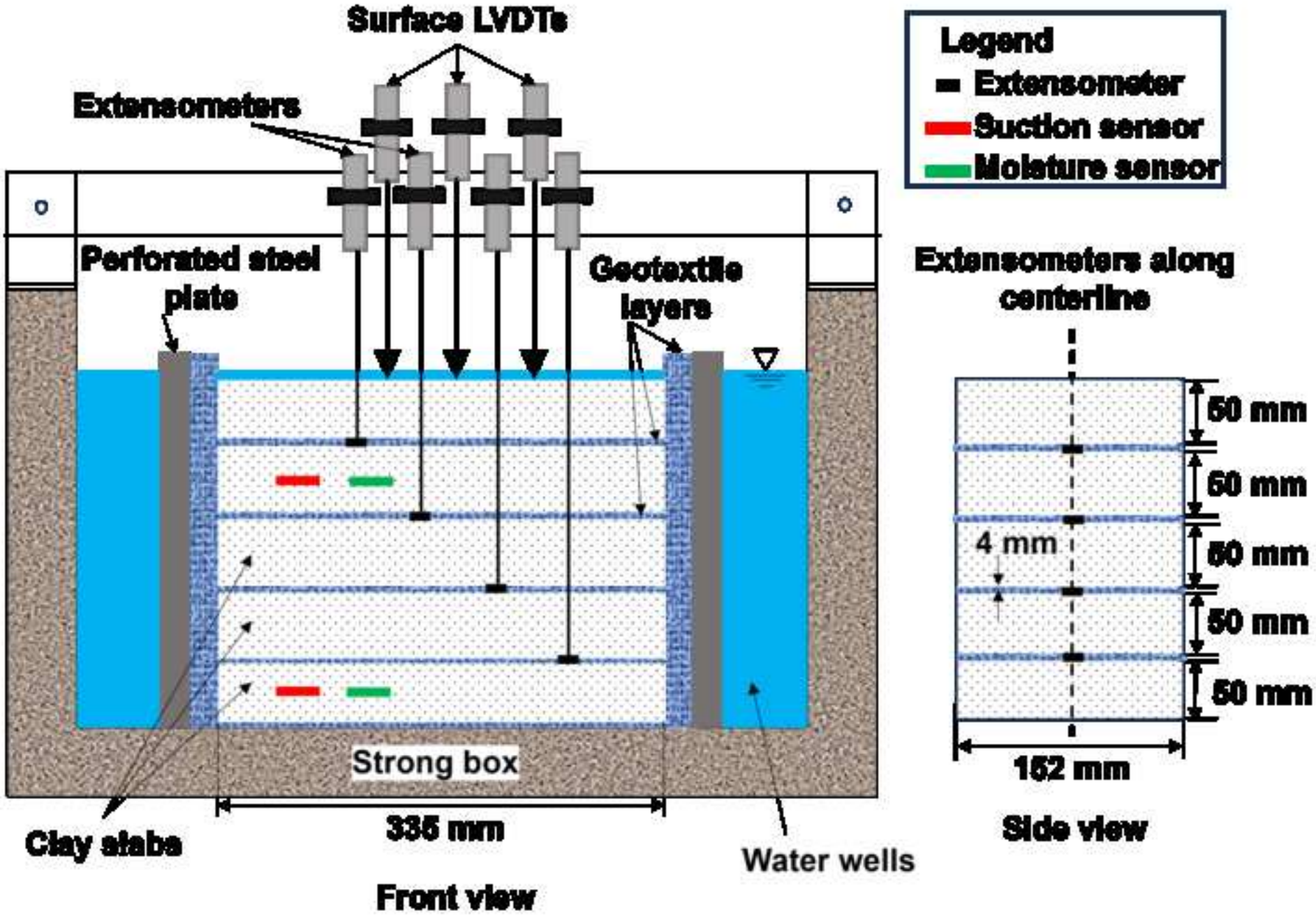


Fig. 2(b)

Click here to access/download;Figure;Fig. 2(b).tif

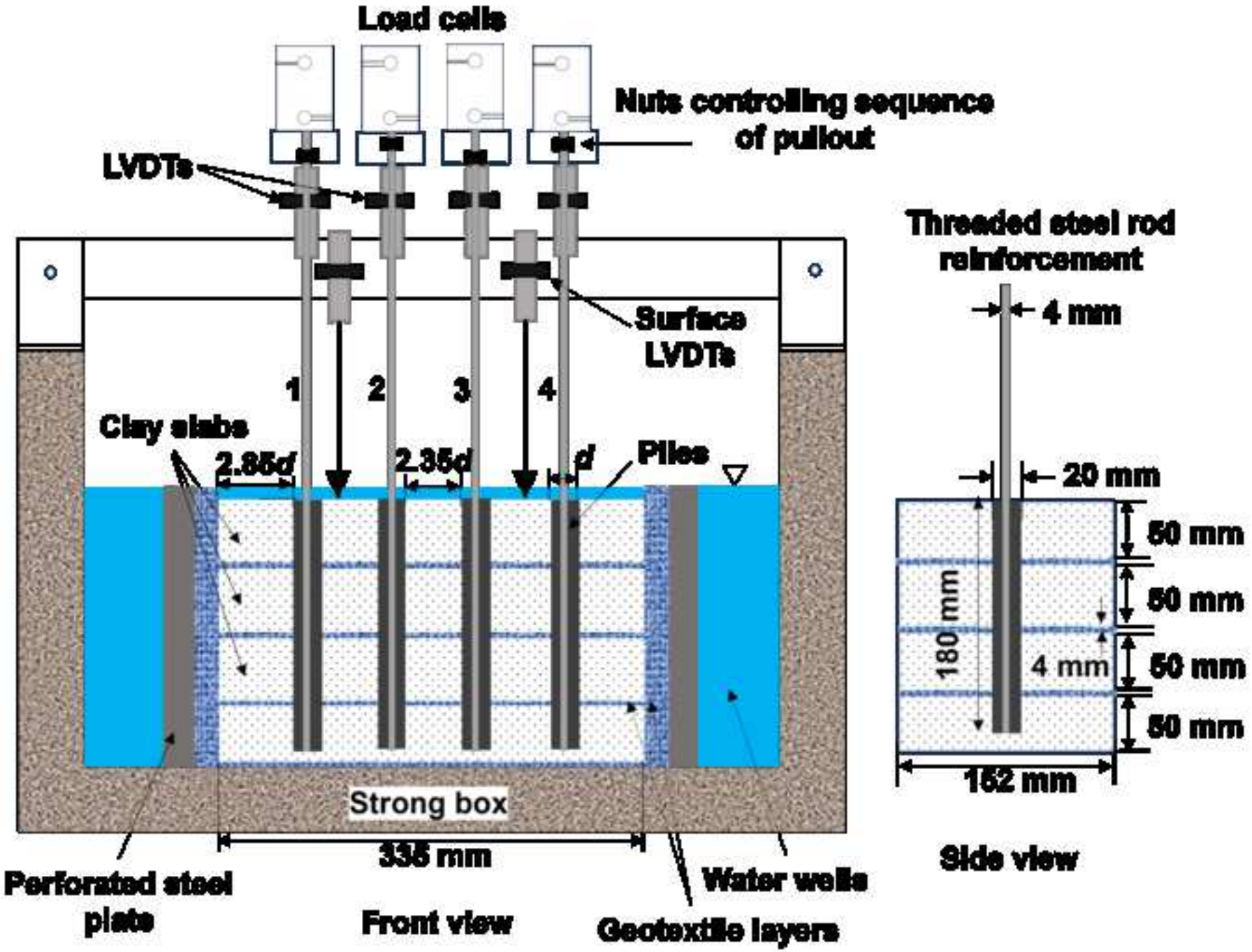


Fig. 3(a)

Click here to access/download;Figure;Fig. 3(a).tif

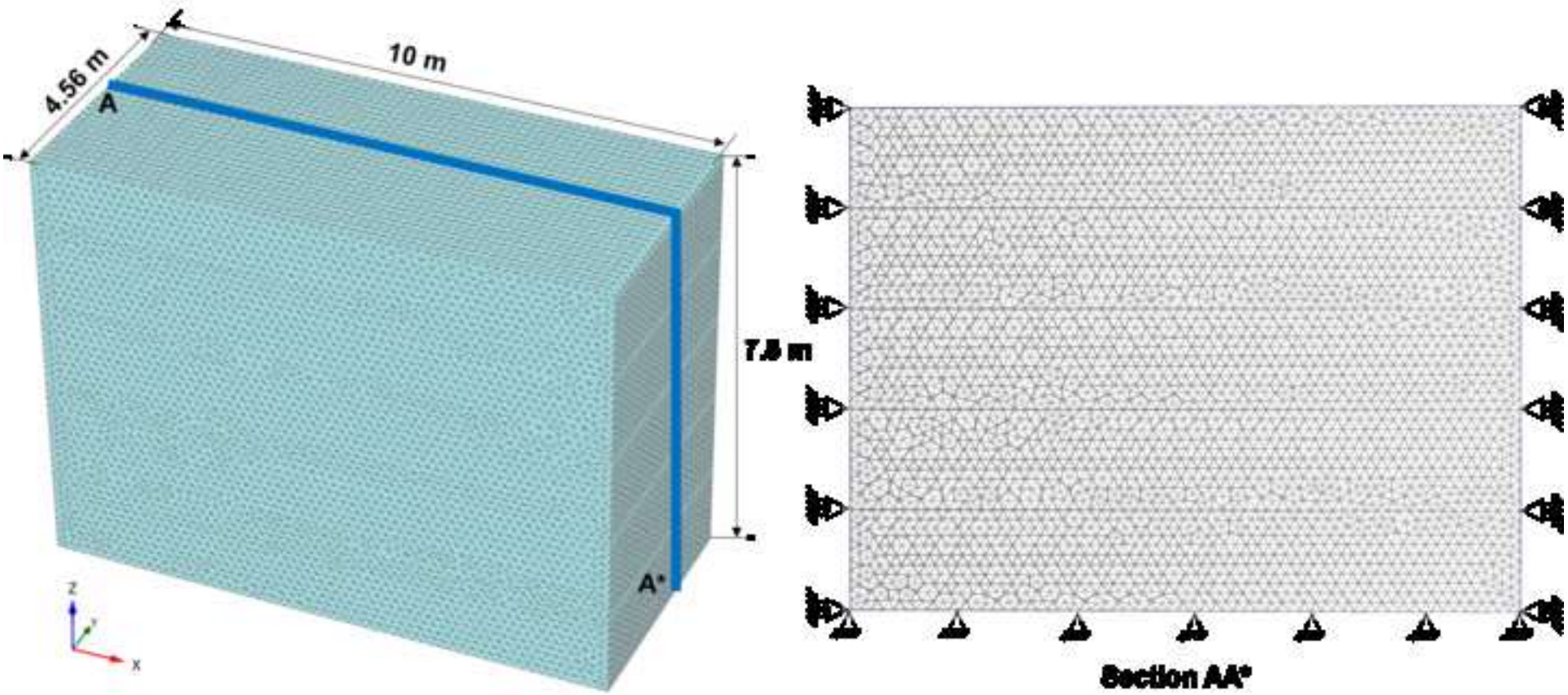


Fig. 3(b)

Click here to access/download;Figure;Fig. 3(b).tif

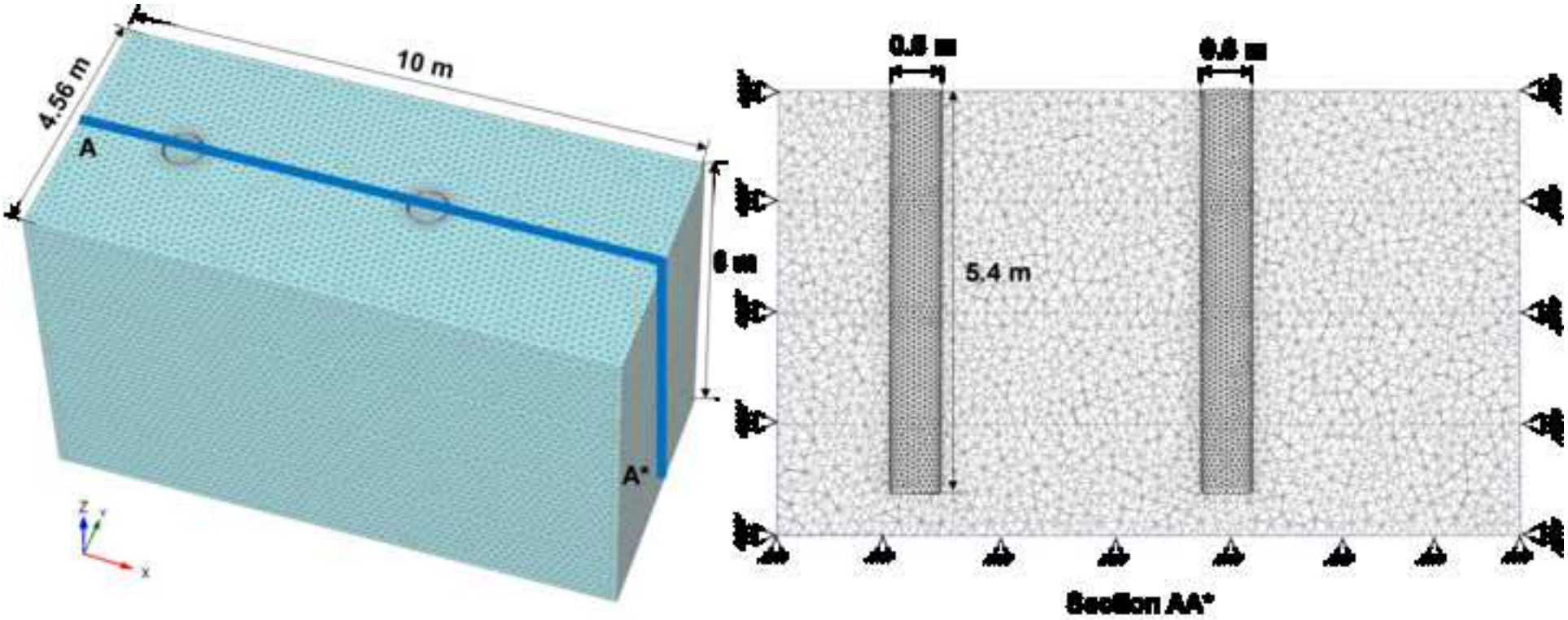


Fig. 4(a)

Click here to access/download;Figure;Fig. 4(a).tif

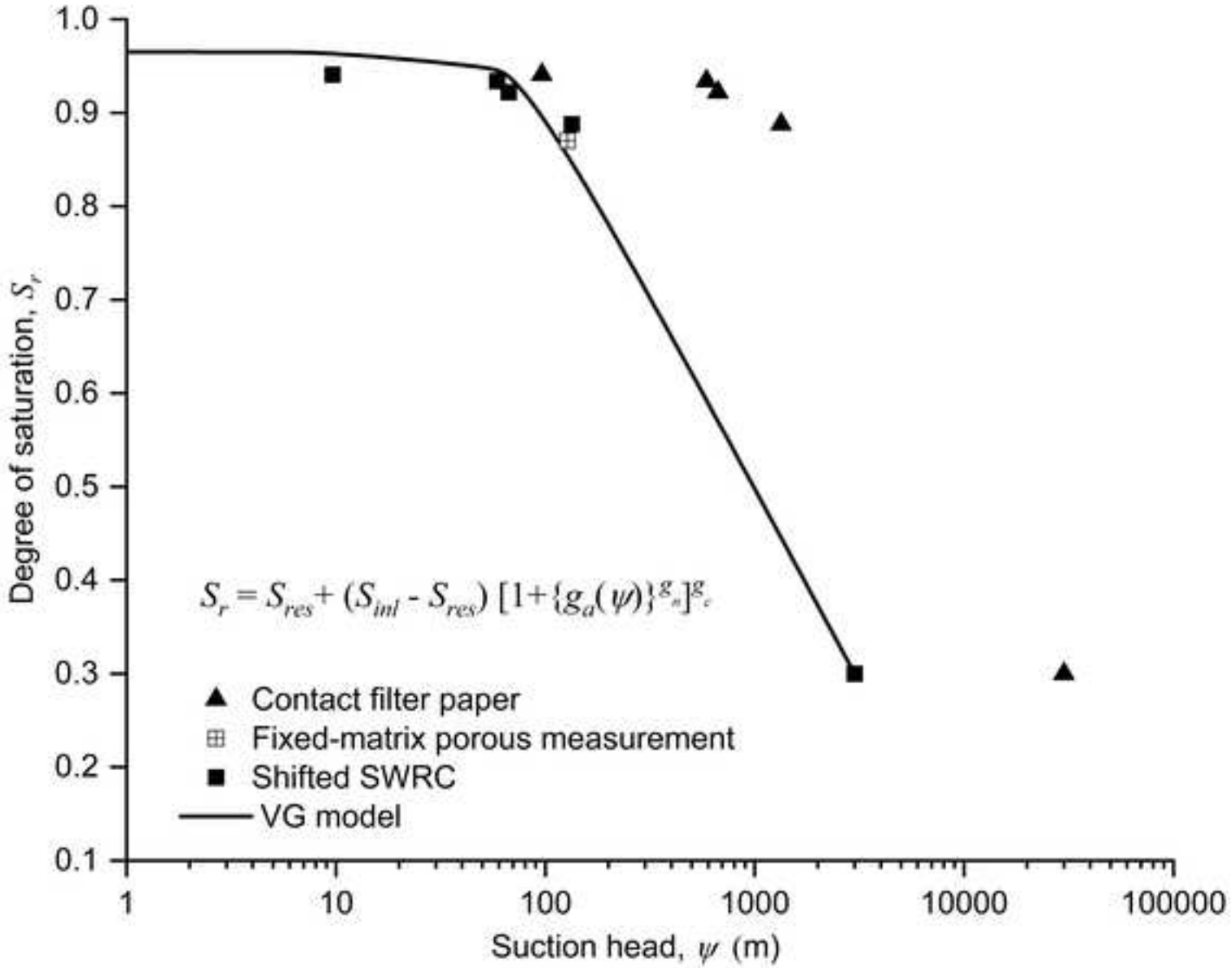


Fig. 4(b)

Click here to access/download;Figure;Fig. 4(b).tif

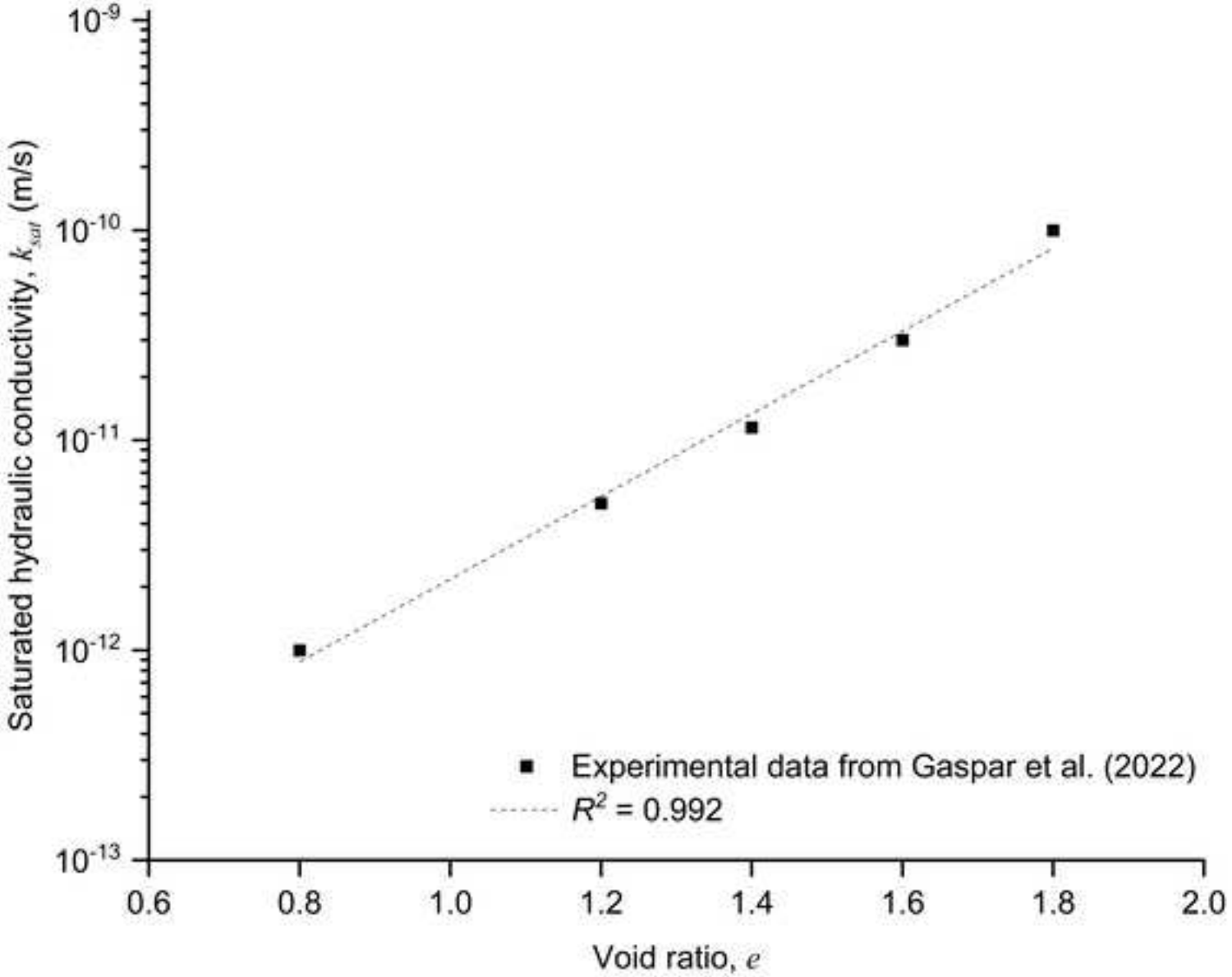


Fig. 5(a)

Click here to access/download;Figure;Fig. 5(a).tif

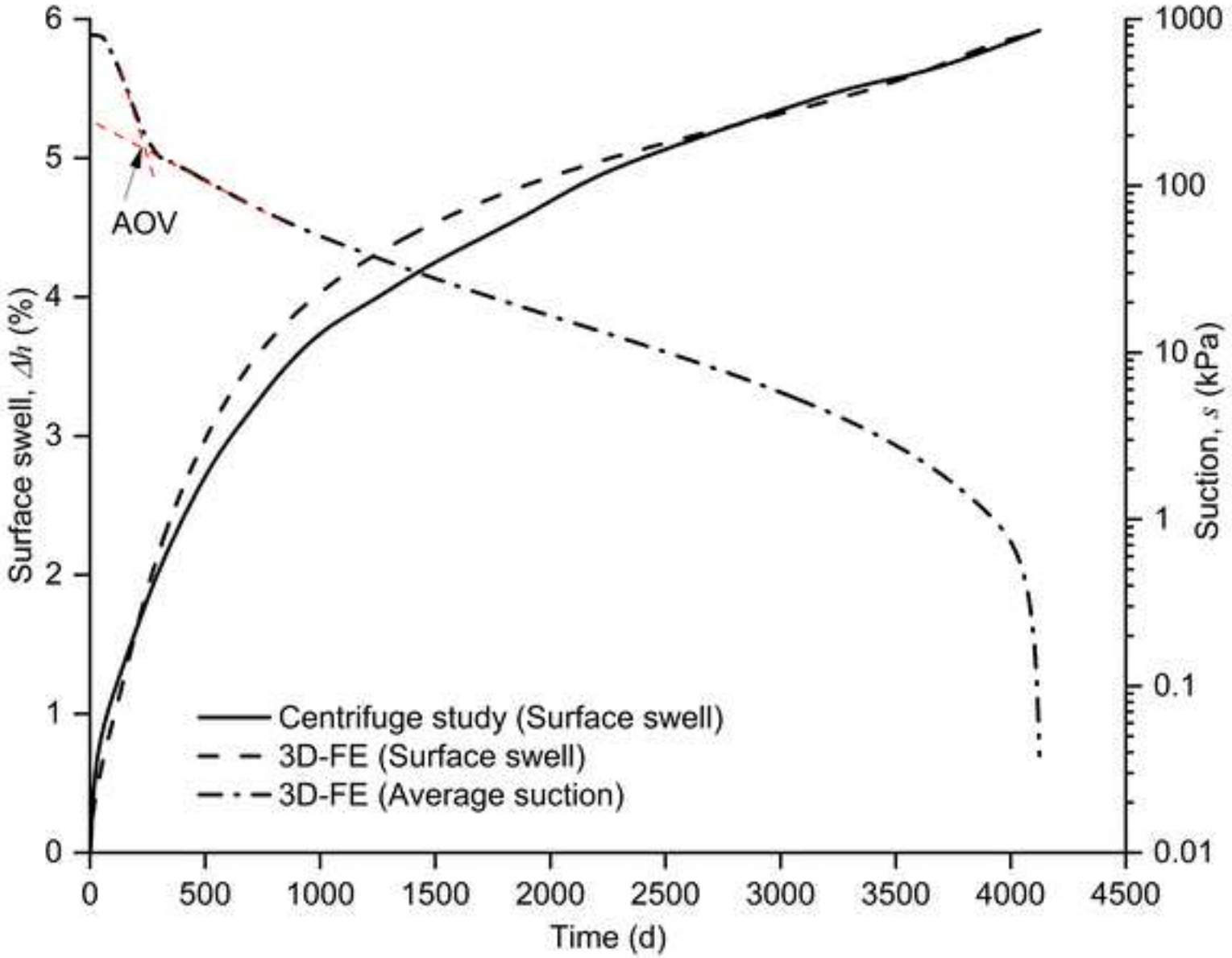


Fig. 5(b)

Click here to access/download;Figure;Fig. 5(b).tif

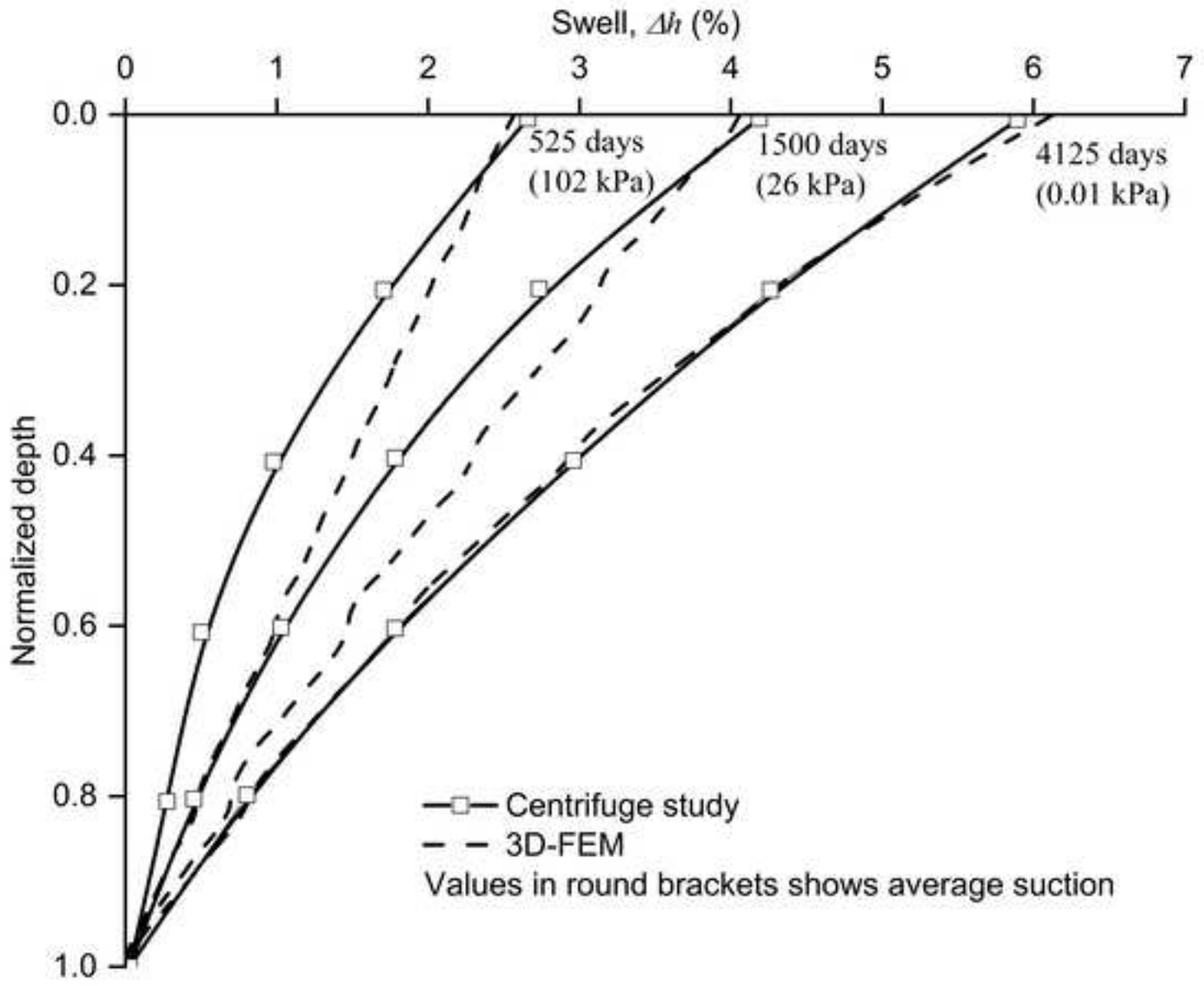


Fig. 6(a)

Click here to access/download;Figure;Fig. 6(a).tif

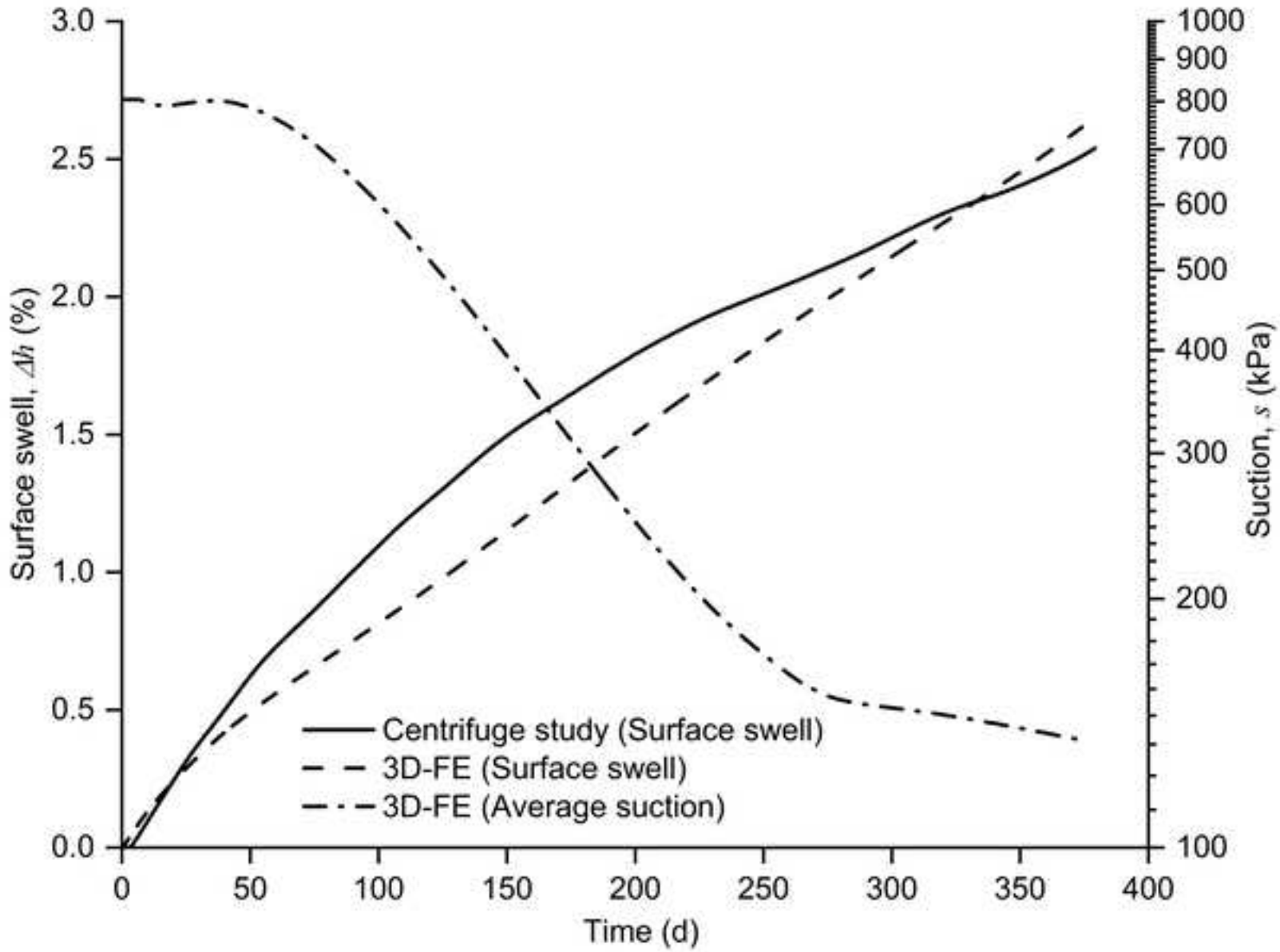


Fig. 6(b)

Click here to access/download;Figure;Fig. 6(b).tif

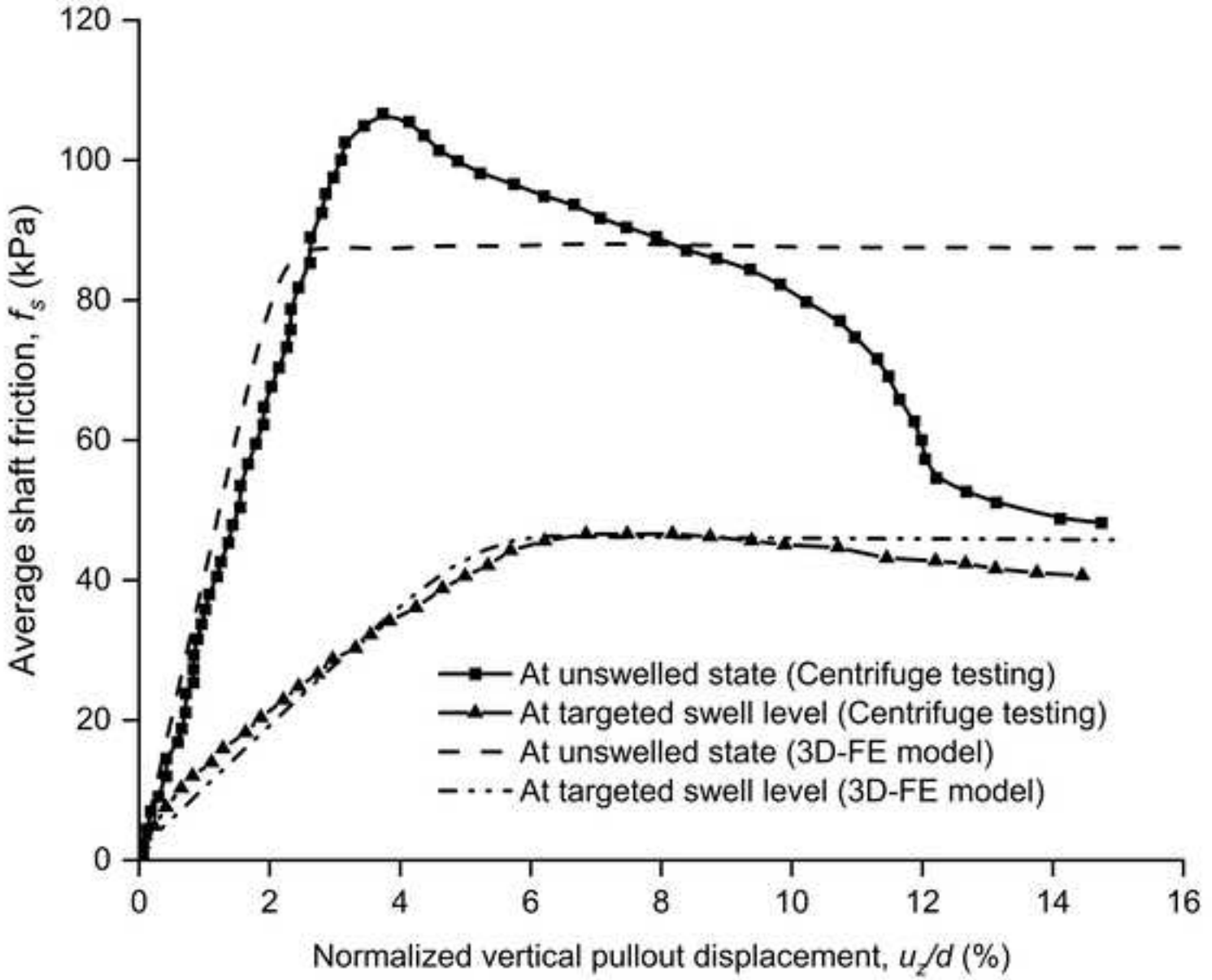


Fig. 7(a)

Click here to access/download;Figure;Fig. 7(a).tif

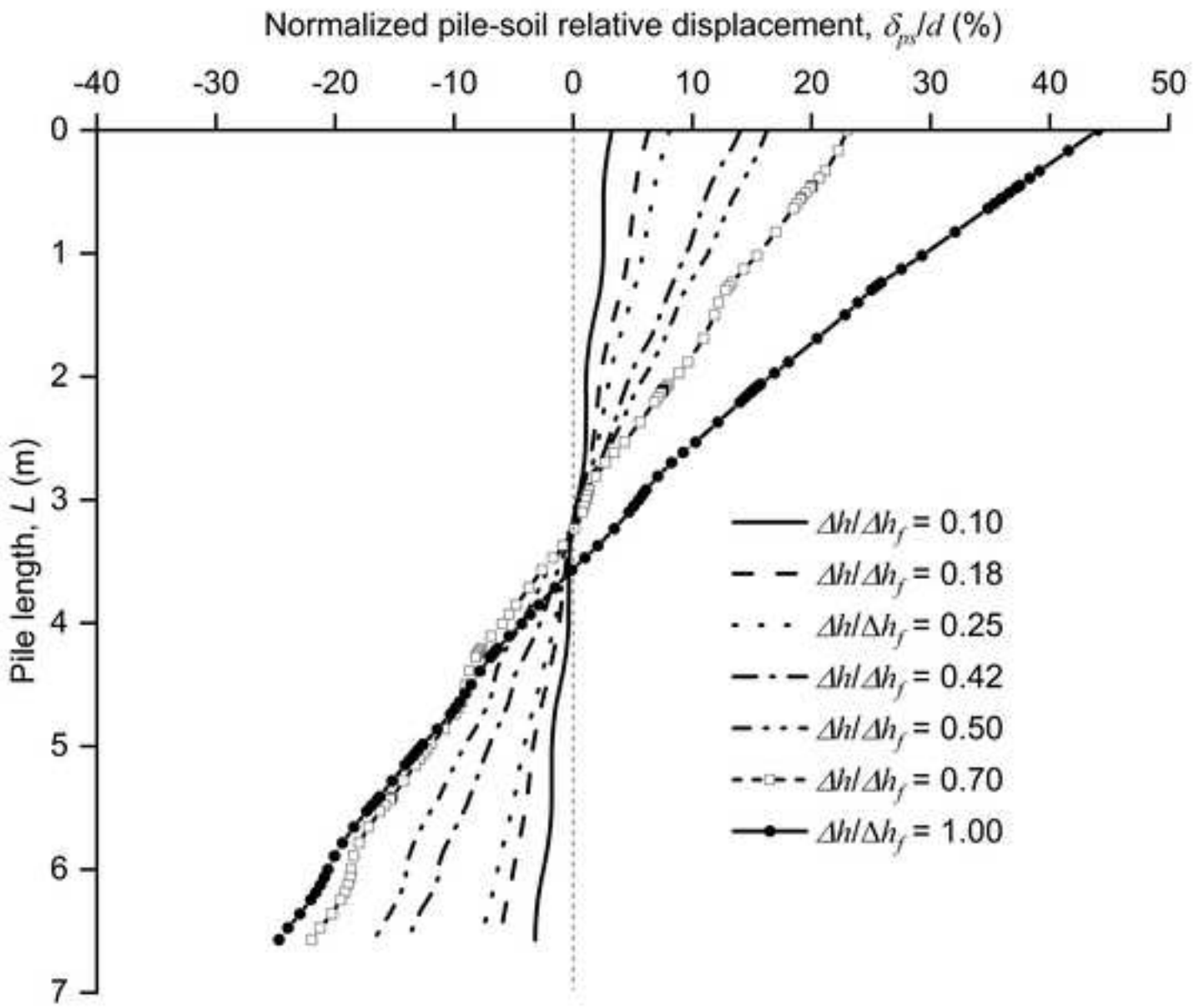


Fig. 7(b)

Click here to access/download;Figure;Fig. 7(b).tif

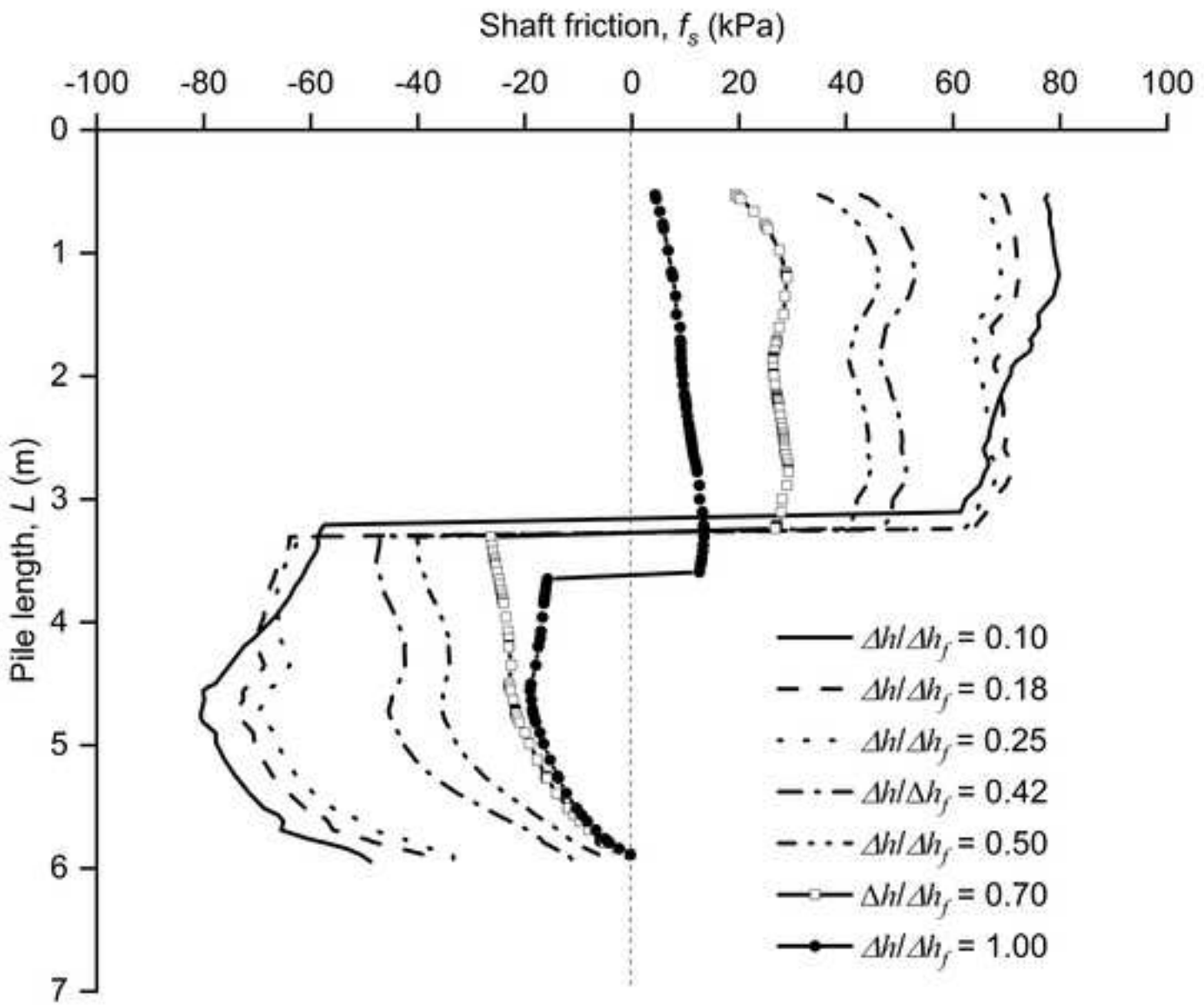


Fig. 7(c)

Click here to access/download;Figure;Fig. 7(c).tif

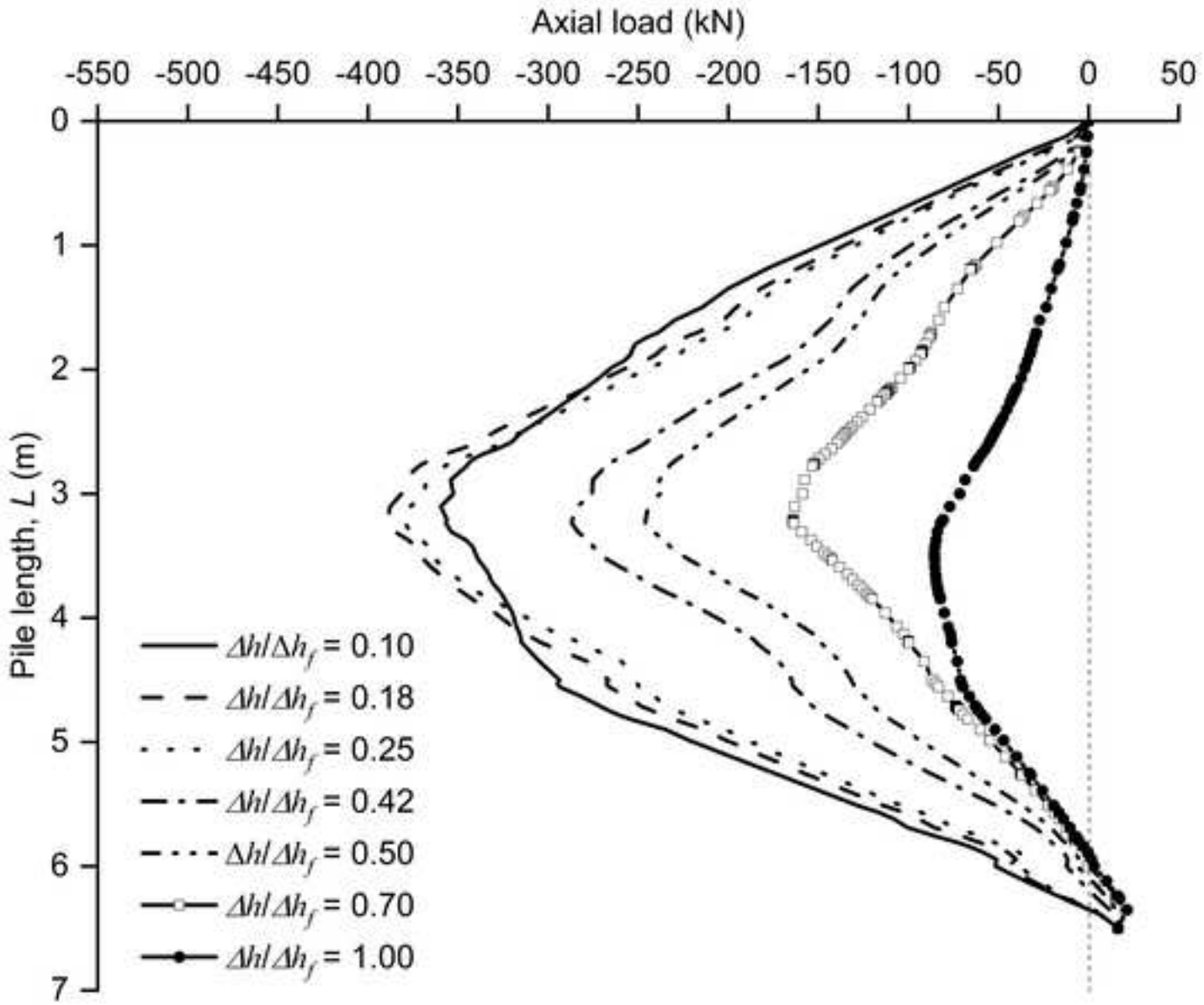


Fig. 8(a)

Click here to access/download;Figure;Fig. 8(a).tif

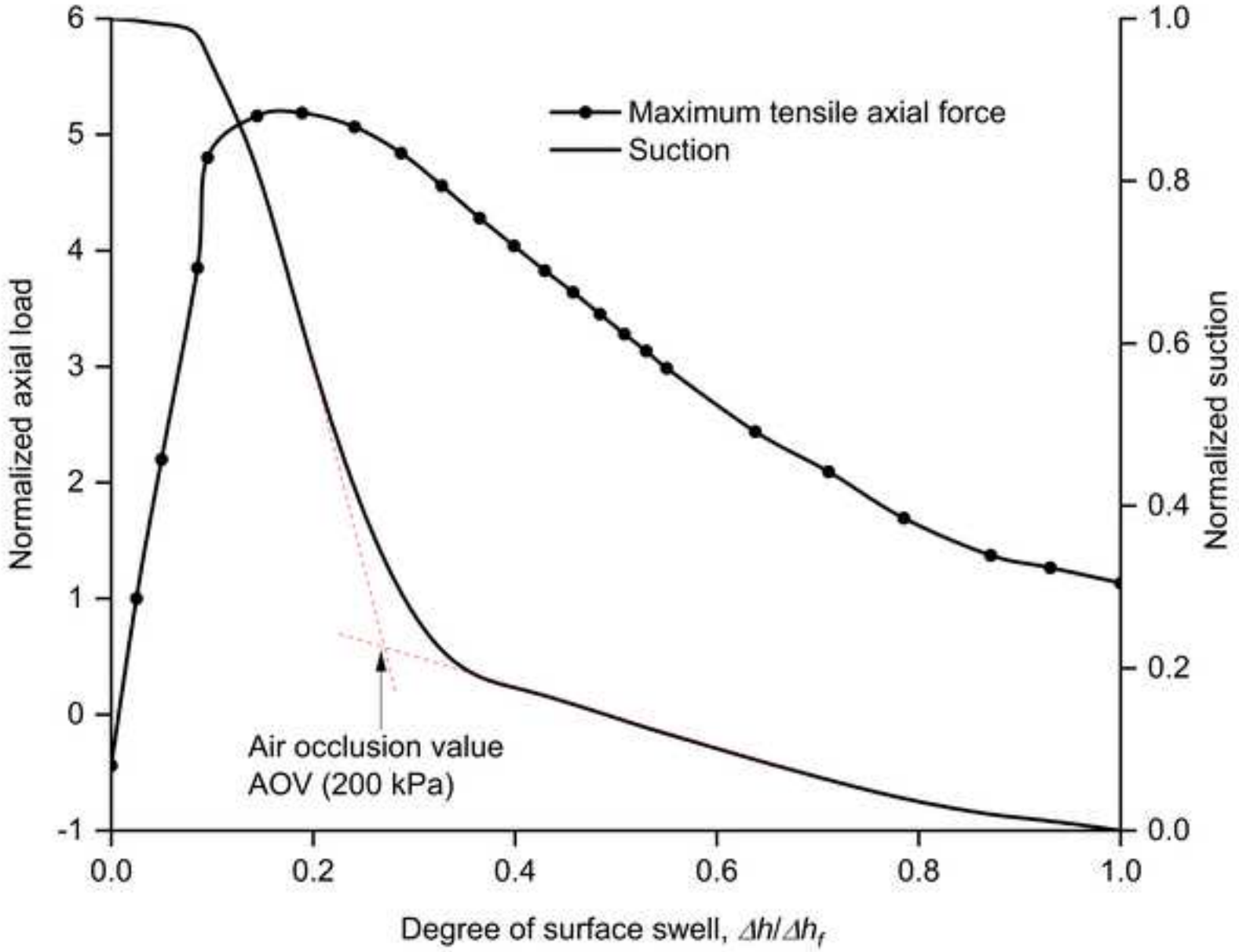


Fig. 8(b)

Click here to access/download;Figure;Fig. 8(b).tif

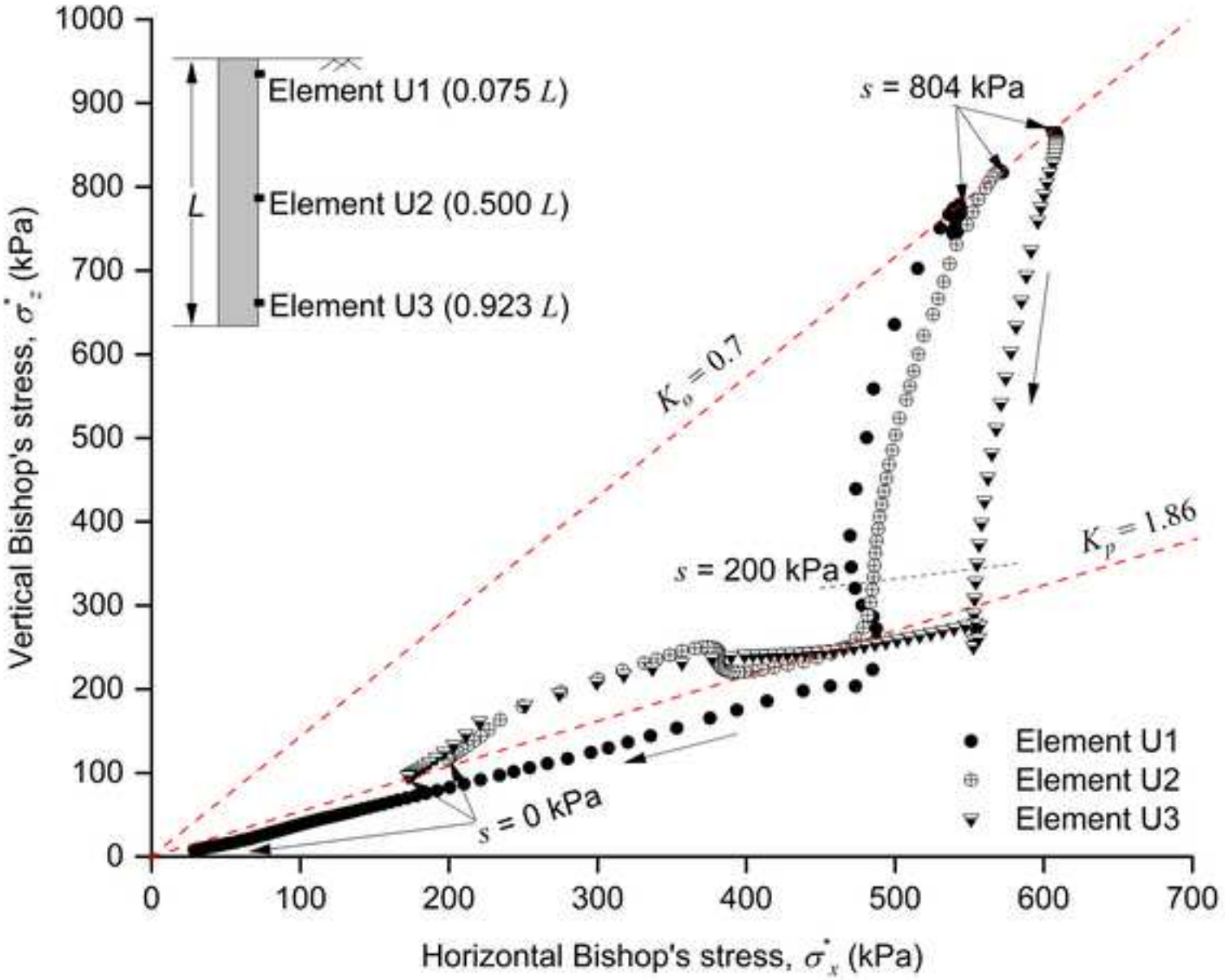


Fig. 9(a)

Click here to access/download;Figure;Fig. 9(a).tif

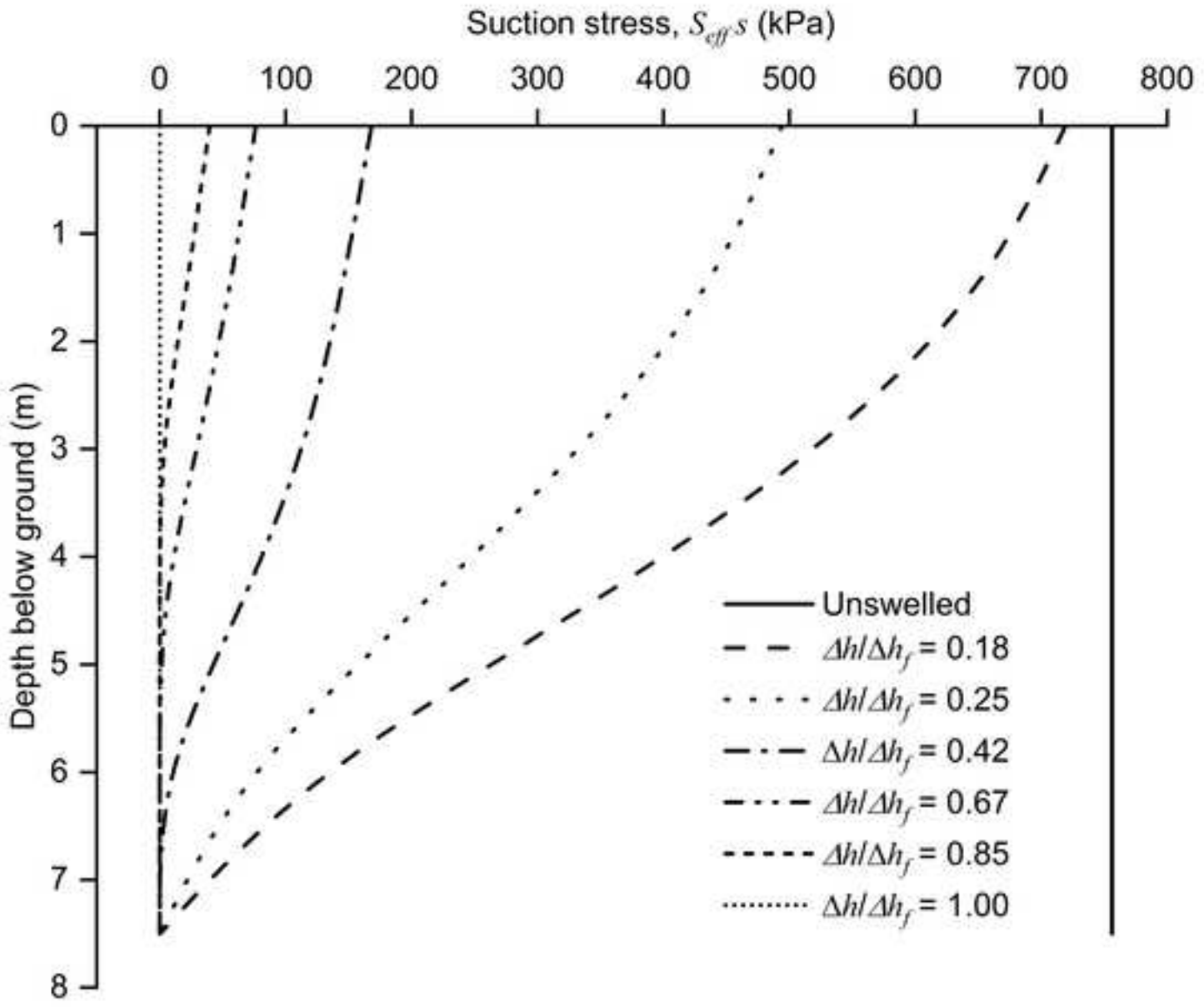


Fig. 9(b)

Click here to access/download;Figure;Fig. 9(b).tif

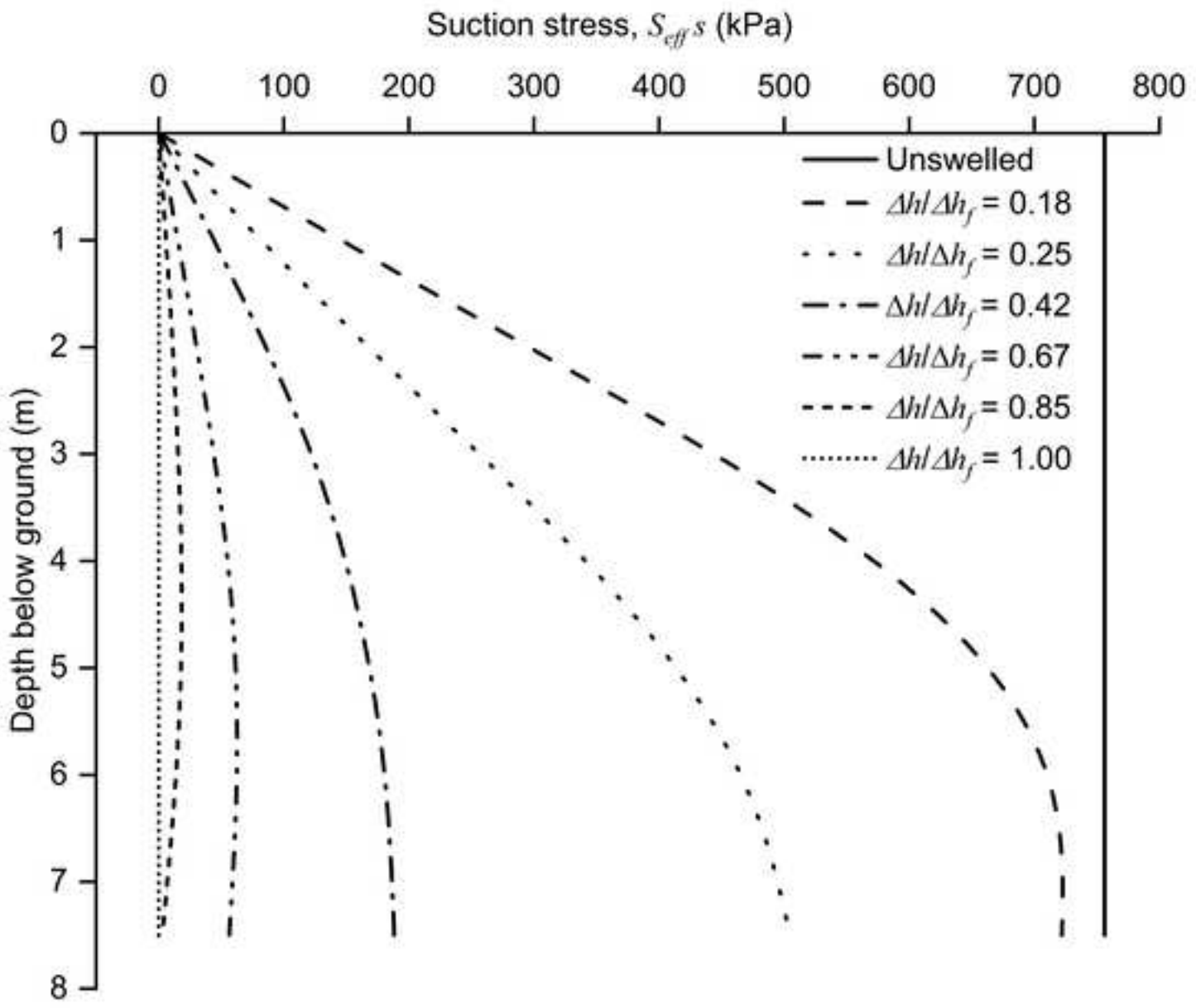


Fig. 10(a)

Click here to access/download;Figure;Fig. 10(a).tif

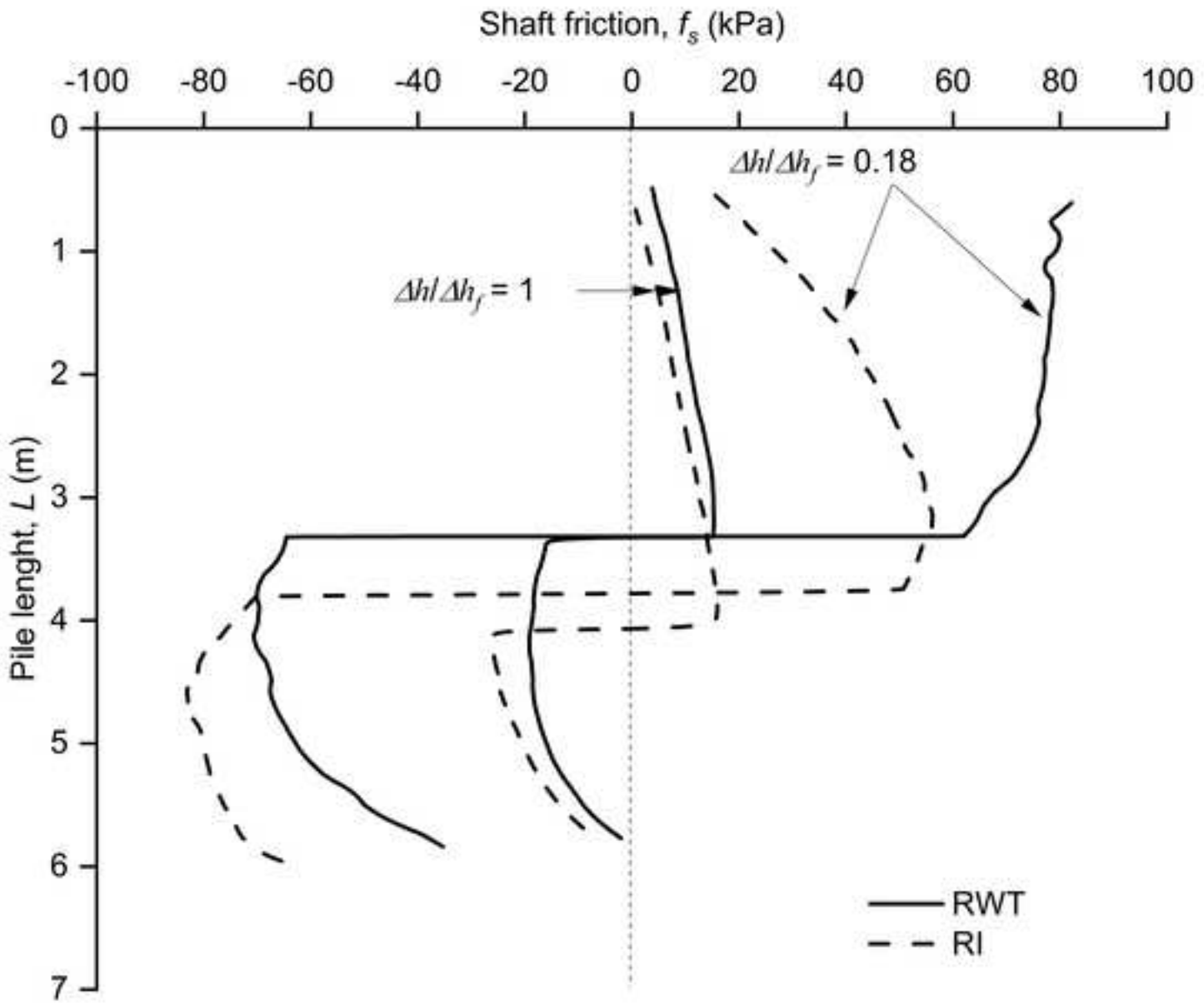


Fig. 10(b)

Click here to access/download;Figure;Fig. 10(b).tif

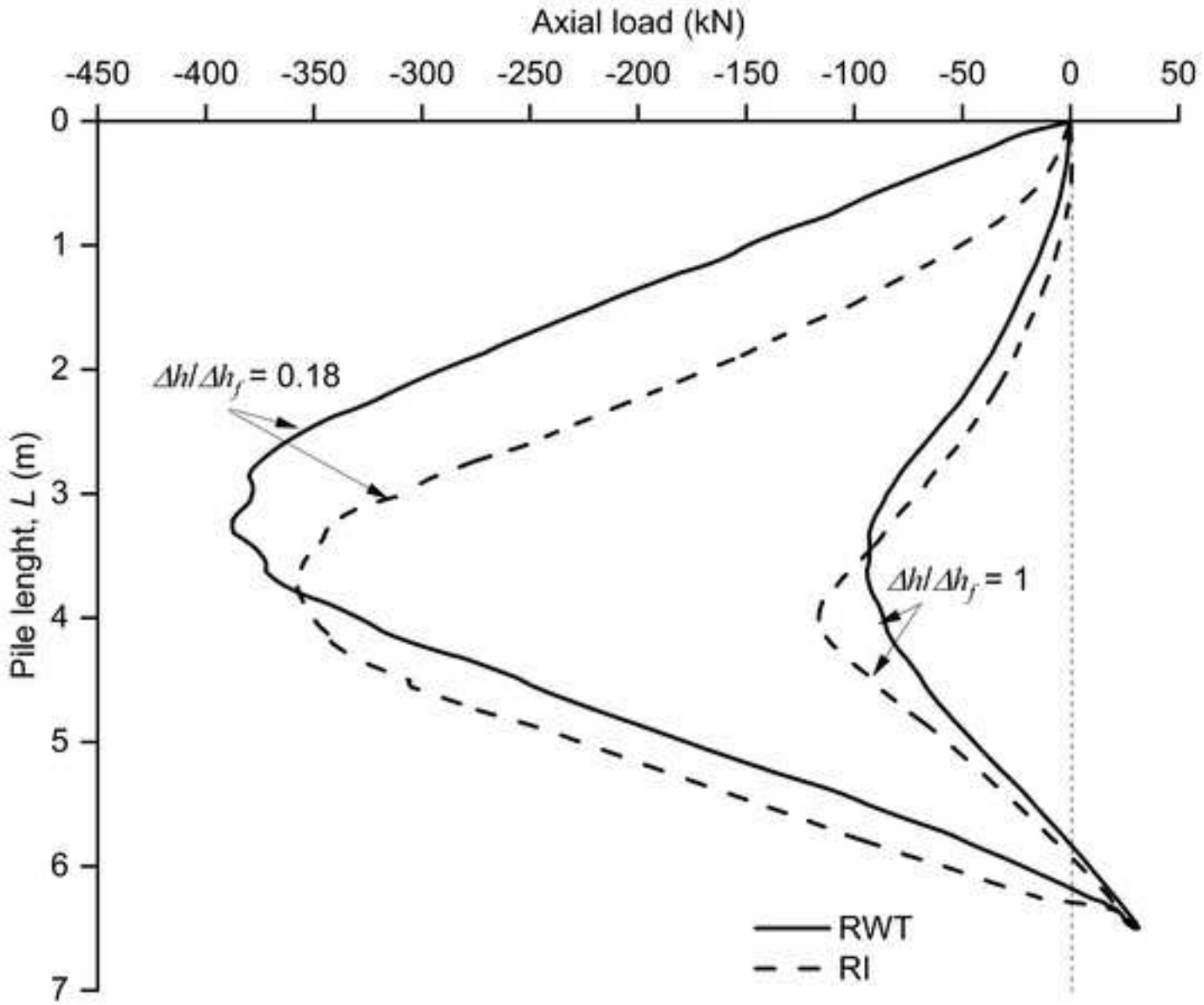


Fig. 11

Click here to access/download;Figure;Fig. 11.tif

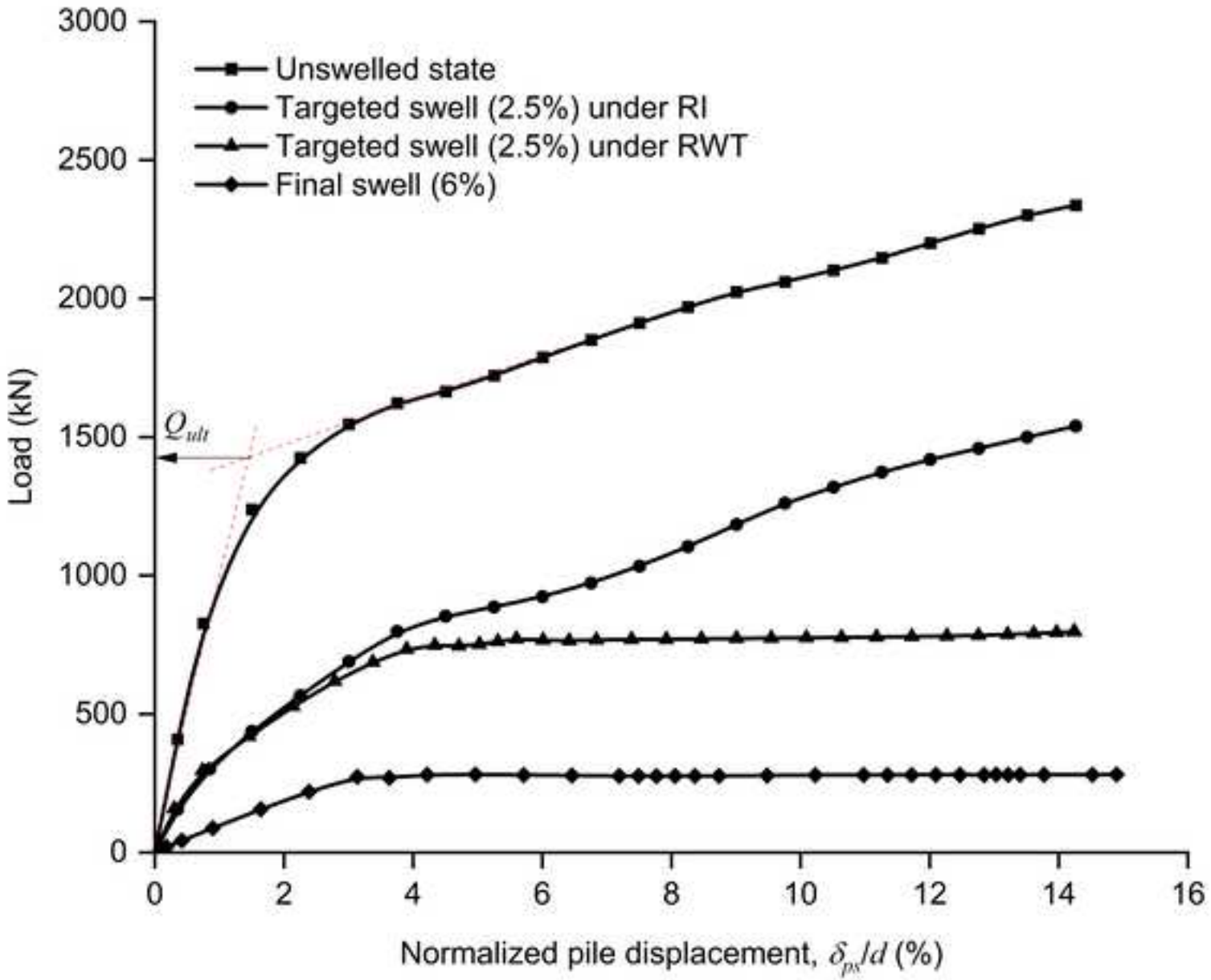


Fig. 12(a)

Click here to access/download;Figure;Fig. 12(a).tif

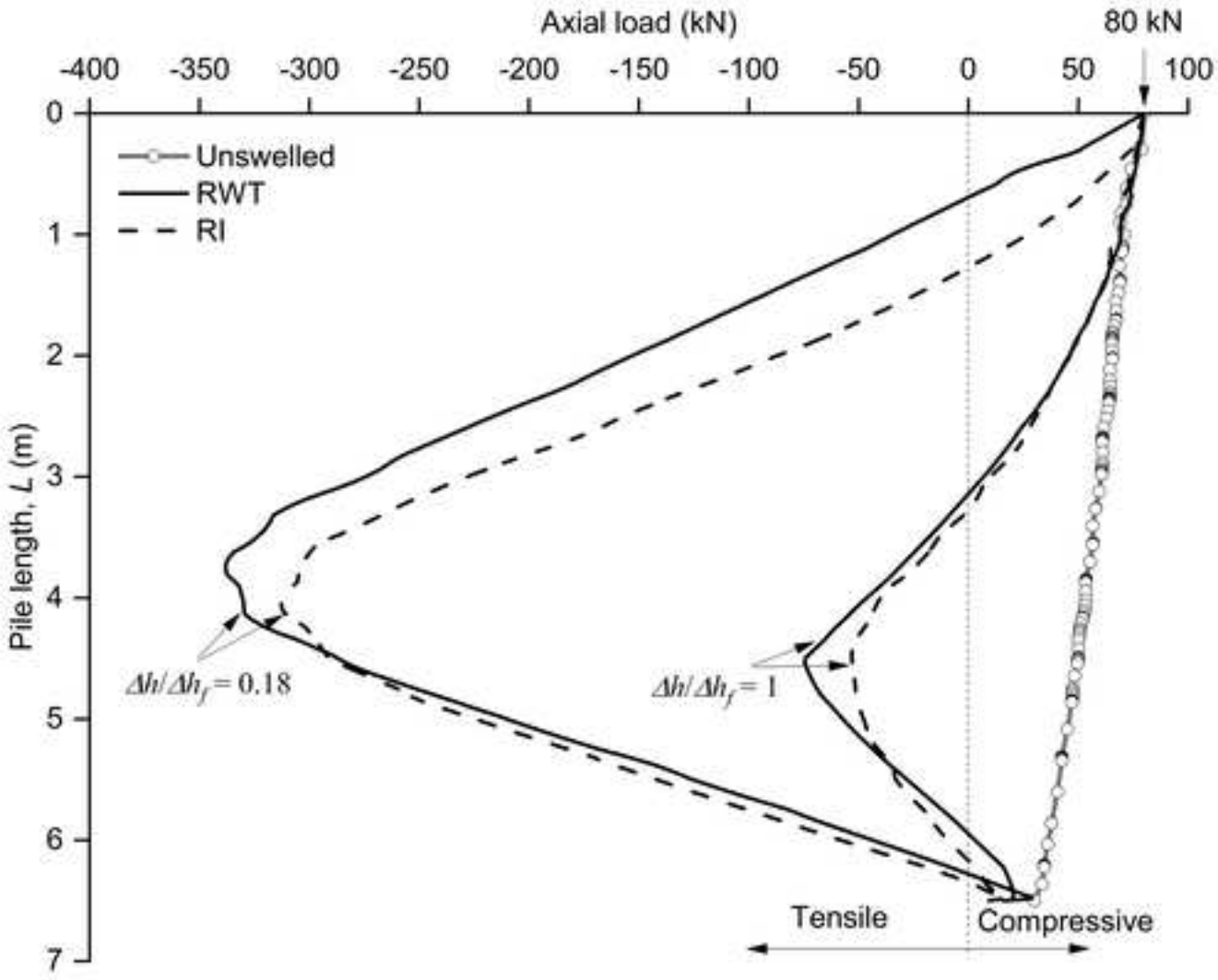


Fig. 12(b)

Click here to access/download;Figure;Fig. 12(b).tif

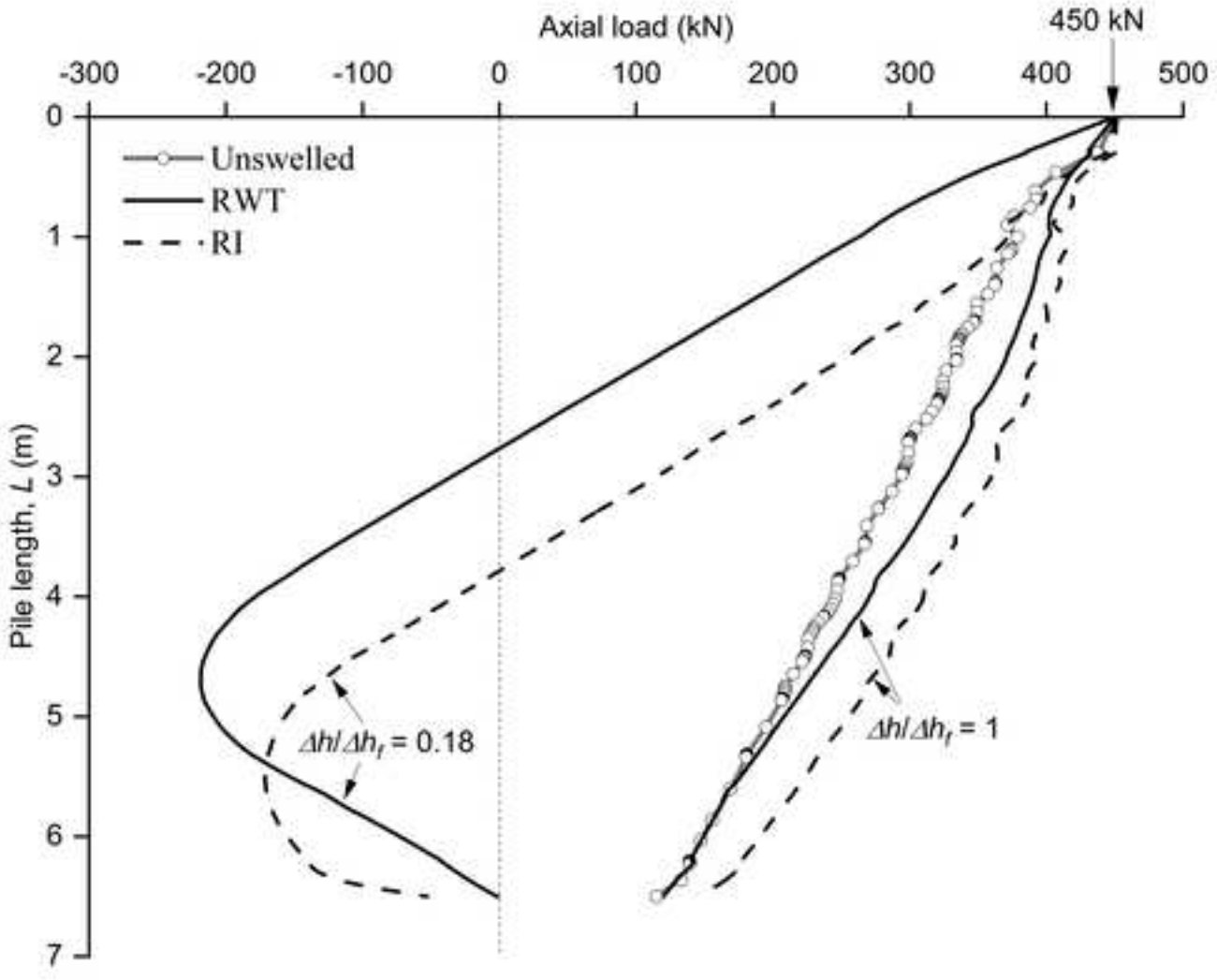


Fig. 12(c)

Click here to access/download;Figure;Fig. 12(c).tif

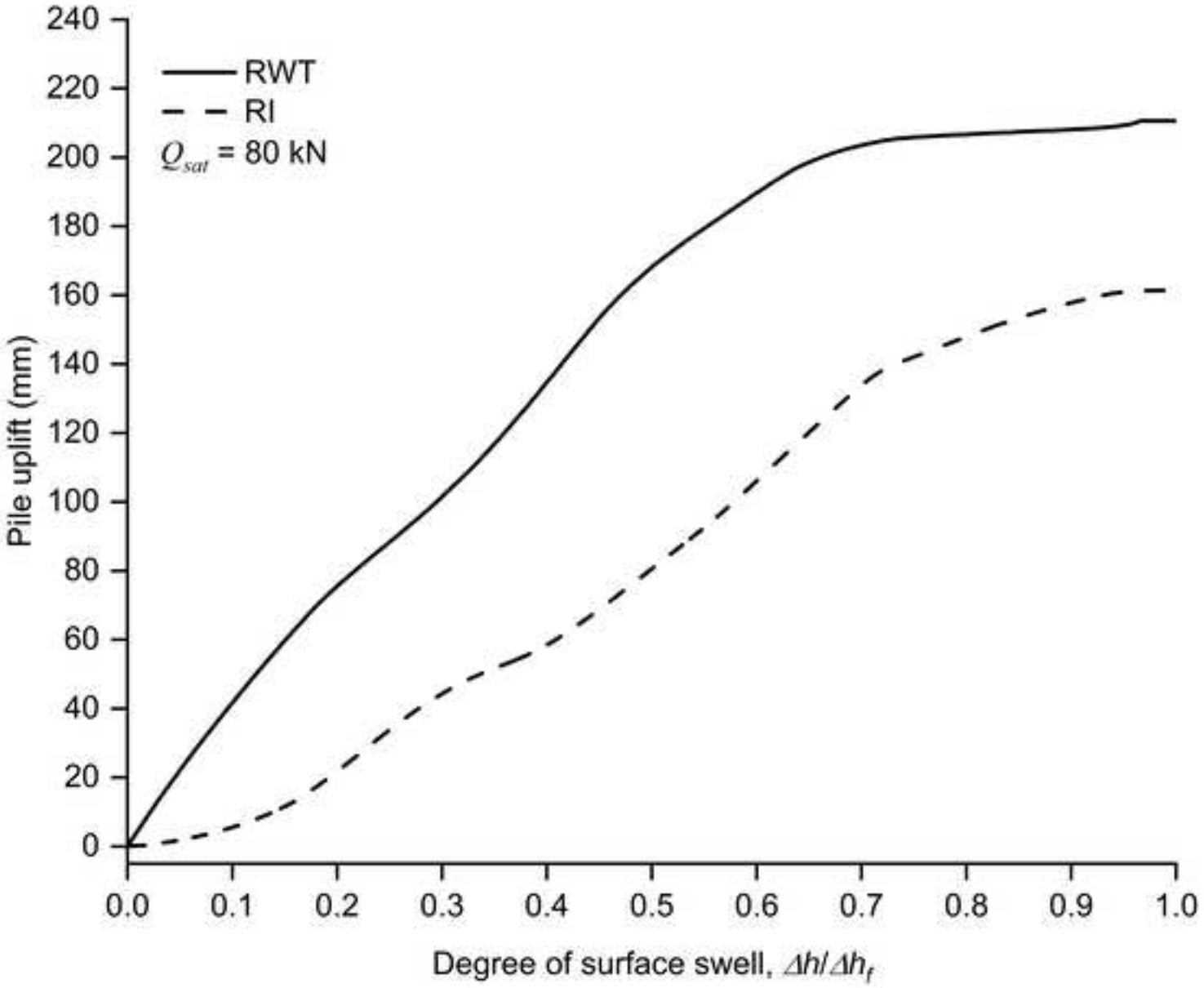
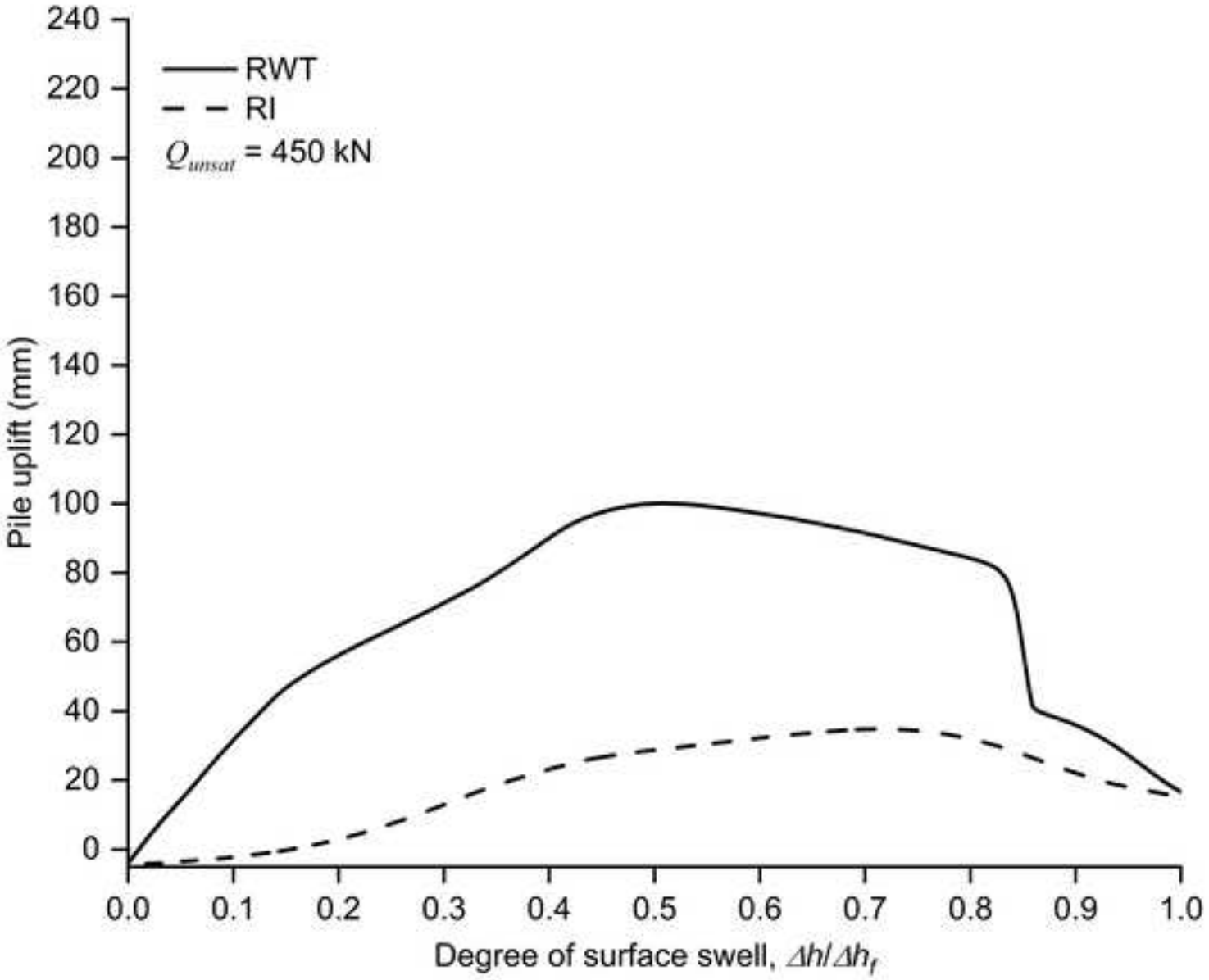


Fig. 12(d)

Click here to access/download;Figure;Fig. 12(d).tif



Click here to access/download
Supplemental Materials File
Supplemental Materials File-GTENG-13906R2.docx

Response to Editors/Reviewers Comments
Click here to access/download;Response to Editors/Reviewers Comments;Response sheet-GTENG-13906R2.docx

Journal Name : **Journal of Geotechnical and Geoenvironmental Engineering**

Manuscript Number : **GTENG-13906R2**

Title : **Impact of suction and swell-induced softening on pile behavior in an unsaturated expansive clay**

Authors : **Sonu Kumar; Ashutosh Kumar; Tiago A.V. Gaspar and Ashraf S. Osman**

Compliance to the comments of the Editor:

Comment: *Dear Professor Kumar: Thank you for your revised submission to the Journal of Geotechnical and Geoenvironmental Engineering. One of the reviewers and the AE have provided additional constructive feedback that may help strengthen your manuscript. The consensus is that the manuscript should be Revised for Editor, which I concur with. A decision on your manuscript is pending your response to the review comments.*

In addition to these comments, I concur with Reviewer 2 that the paper is currently too long. Please make every effort to make certain text more concise and move less relevant figures to a Supplemental Appendix, which will accompany the paper online at the ASCE Library website. For example, Figs. 10c and 10d are ready candidates for moving to the Supplemental Appendix, and other figures can be combined into more efficient multi-subfigure figures.

Please note that a failure to adequately address these and the outstanding comments below may result in your submission being declined.

To proceed please provide a point-by-point response to each reviewer comment, and provide a marked copy with edits to aid in the re-review process. Once revised your manuscript will be assessed by myself and the Associate Editor. Please contact me if you have any questions.

Thanks for your continued interest in the Journal of Geotechnical and Geoenvironmental Engineering.

Reply: The authors are grateful to the Editor for providing us with the opportunity to revise the manuscript based on the Reviewer 1 and the AE minor comments. All the comments and suggestions have now been addressed, and suitable modifications have been made in the revised manuscript. We have now made a great effort to shorten the manuscript and created Supplemental Materials to transfer some of the information of the main manuscript while maintaining the clarity. As suggested, Figures 10c and 10d are now presented within the Supplemental Materials. In addition, we have now moved the calibration of the Barcelona Basic Model parameters within the Supplemental Materials. The accompanying annotated revised copy of the manuscript shows all the changes made according to the reviewers' comments. We hope that the Editor will find all the comments in proper order. Our detailed responses to the comments are summarised below.

Compliance to the comments of the Associate Editor:

Comment: *The authors have addressed the comments and revised the manuscript for the most part. One of the reviewers have a couple of comments that I think the clarification with regards to the numerical modeling is warranted. Please consider this, revise, and resubmit.*

Reply: The authors sincerely thank the Associate Editor's acknowledgment that our responses have adequately addressed most of the comments previously raised. We thank the Associate Editor for providing feedback on our manuscript based on the reviewer's comments and for giving us the opportunity to revise the work again. We have now revised the manuscript. A point-by-point rebuttal to the reviewers' comments is provided below.

Compliance to PEER review comments:

Reviewer #1:

Comment: *The authors have thoroughly addressed most of the comments. In the reviewer's opinion, the paper could be accepted for publication after addressing the following points:*

Reply: The authors sincerely thank the reviewer for recommending the acceptance of this manuscript following minor revisions. We have revised the manuscript accordingly. A point-by-point response is appended below.

Comment: *1. Length. The revised version is only 200 words shorter than the original submission. At over 45 pages, it significantly exceeds the recommended length of 30 pages outlined in the author guidelines (https://ascelibrary.org/author-center/journal#). The authors are encouraged to make a substantial effort to streamline the manuscript.*

Reply: Thank you for raising this important concern regarding the manuscript length. We acknowledge that the revised version initially remained above the recommended page limit. In line with the Editor's recommendation to streamline the manuscript, we have now transferred element scale calibration of saturated state parameters (Figure 4) and other parameter estimations of the BBM (Figure 5c&d) to the Supplemental Materials section. This adjustment preserves the technical completeness of the paper while improving conciseness in the main body. As a result, the overall manuscript length has been further reduced by approximately 718 words. We believe that the revised manuscript now presents the key findings and methodology more efficiently without compromising technical quality and appreciate the Editor's guidance in this matter.

Comment: *2. Saturated permeability. This is more of a curiosity. The authors stated that the fissured nature of the clay was implicitly accounted for in the numerical modelling, including the assigned permeability. However, the k_{sat} value reported in Table 3 (approximately 10-12 m/s), derived from experimental data, seems very low for an average value that includes the effect of fissures. Could the authors provide further clarification on this point?*

Reply: Thank you for raising this concern. At first glance, it can be appreciated that the selection of k_{sat} = 10^{-12} m/s may seem a bit low for a value that is supposed to incorporate fissuring. To understand such a selection, it is worth considering the range over which hydraulic conductivity would vary during the wetting process. For an unsaturated fissured clay, initially, the bulk hydraulic conductivity will be significantly greater than the saturated hydraulic conductivity (k_{sat}) of the intact material. However, this value will only be applicable momentarily because infiltration will close up the fissures due to swelling. At the instance that fissures have been closed, the hydraulic conductivity (k_{unsat}) governing infiltration into unsaturated clay mass will be several orders of magnitude lower than k_{sat}. However, as wetting progresses, the void ratio will increase and suction will reduce, leading to a progressive increase in k_{unsat}.

A more rigorous way of accounting for this sort of behavior would be to incorporate a dual structure model which allows for an independent control over macro- and micro-structural hydraulic conductivity (as presented by Zdravković et al. 2018). However, such models are not facilitated in PLAXIS. For this reason and given that the hydraulic conductivity would vary from several orders of magnitude above to several orders of magnitude below k_{sat}, the selection of an intermediate k_{sat} was deemed appropriate. The validity of this selection was further reinforced by the fact that the numerical model accurately reproduced the time-dependent

swelling observed during the diffusion process in the centrifuge tests with the adopted value of k_{sat}. We have now added this justification within the revised manuscript.

Reference:

Zdravkovic, L., Tsiampousi, A., and Potts, D.M. 2018. On the modelling of soil-atmosphere interaction in cut and natural slopes. In Proceedings of the 7th International Conference on Unsaturated Soils, Hong Kong, 3–5 August 2018.

Revised text now read as:

It should be noted that in fissured clay, the initial hydraulic conductivity may significantly exceed k_{sat} due to open fissures. However, during a swell process, this higher hydraulic conductivity is only momentarily applicable as swelling rapidly closes fissures, causing conductivity to drop sharply by several orders of magnitude to much lower unsaturated levels (k_{unsat}). With continued wetting, increased void ratio and reduced suction gradually raise k_{unsat}. Due to the high variability in hydraulic conductivity throughout swell, k_{sat} was chosen as a representative intermediate value, an approach validated by the accurate simulation of swelling over time in the 3D-FE model in comparison to centrifuge test (see next section).

Comment: 3. Figure 5. There is a typo in the legend. Please amend it.

Reply: The authors sincerely thank the reviewer for pointing out the typos in Figure 5. We have now revised Figure 5b and Figure 5c.

Reviewer #2:

Comment: *All the comments from this reviewer have been sufficiently addressed.*

Reply: The authors sincerely appreciate the reviewers' acknowledgment that our responses have adequately addressed the comments previously raised. We are grateful for the constructive feedback provided by the reviewer which has significantly contributed to enhancing the quality of the manuscript.

Click here to access/download
Track Changes Version
Annotated Manuscript-GTENG-13906R2.docx